

A COMPARISON BETWEEN EXPERIMENTAL ELECTRON
CAPTURE DATA AND A MODIFIED BRINKMAN-KRAMERS CALCULATION

by

JAMES ANDREW GUFFEY

B. S., University of Missouri-St. Louis, 1972

A MASTER'S THESIS

submitted in partial fulfillment of the

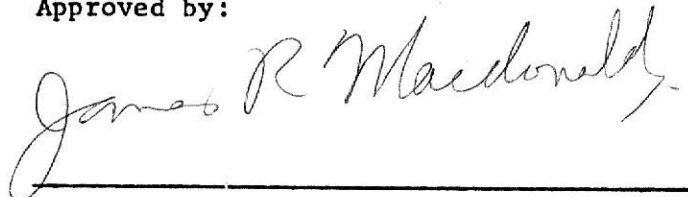
requirements for the degree

MASTER OF SCIENCE

Department of Physics

KANSAS STATE UNIVERSITY
Manhattan, Kansas
1974

Approved by:



Major Professor

LD
2668
T4
1974
684
C. 2
Document

TABLE OF CONTENTS

List of Figures	iii
List of Tables	v
Acknowledgements	vi
I. Introduction	1
II. Electron Capture Experiments:	11
A. Total Capture for Protons	11
B. Total Single Capture for Heavy Bare Projectiles	15
C. Capture From a Particular Shell of the Target by Protons	20
D. Capture to a Particular Shell(s) of the Projectile	24
III. Results and Discussion:	28
A. Total Capture for Protons	28
B. Total Single Capture for Heavy Bare Projectiles	35
C. Capture From a Particular Shell of the Target by Protons	44
D. Capture to a Particular Shell(s) of the Projectile	48
IV. Summary and Conclusion	52
Appendix	54
List of References	58

**THIS BOOK
CONTAINS
NUMEROUS PAGES
WITH THE ORIGINAL
PRINTING BEING
SKEWED
DIFFERENTLY FROM
THE TOP OF THE
PAGE TO THE
BOTTOM.**

**THIS IS AS RECEIVED
FROM THE
CUSTOMER.**

LIST OF FIGURES

Number	Description	Page
1	Calculated Electron Capture Cross Section versus Fluorine Principal Quantum Number	8
2	Schematic of the Apparatus for the Determination of Total Electron Capture Yields for Protons in Gases	12
3	Flow Chart for the Analysis of the Single Electron Capture Cross Sections for Protons	14
4	Schematic of the Apparatus for the Determination of Electron Capture Yields for Heavy Bare Projectiles.	16
5	Particle Detector Counts versus Channel Number for Fluorine on Nitrogen.	17
6	Flow Chart for the Analysis of the Electron Capture Cross Sections for Heavy Projectiles	18
7	Schematic of the Apparatus for the Determination of the Coincidences Between Electron Capture From the K Shell of the Gas Target by Protons	21
8	Flow Chart for the Analysis of the Single Capture Cross Sections for the Coincidence Experiment.	23
9	Schematic of the Apparatus for the Determination of Projectile K Shell X-Ray Yields in Gases	25
10	Flow Chart for the Analysis of the Cross Sections for X-Ray Production	27
11	Total Single Capture Cross Section versus Projectile Energy for Protons on Hydrogen.	29
12	Total Single Capture Cross Section versus Projectile Energy for Protons on Helium	30
13	Total Single Capture Cross Section versus Projectile Energy for Protons on Nitrogen	31
14	Total Single Capture Cross Section versus Projectile Energy for Protons on Neon	32
15	Total Single Capture Cross Section versus Projectile Energy for Protons on Argon	33

Number	Description	Page
16	Total Single Capture Cross Section versus Projectile Energy for Fluorine on Argon	38
17	Calculated-to-Experimental Single Capture Cross Section Ratios versus Projectile Energy for Z_1^{+q} -Ar	39
18	Calculated-to-Experimental Single Capture Cross Section Ratios versus Projectile Energy for Z_1^{+q} -Kr	40
19	Calculated-to-Experimental Single Capture Cross Section Ratios versus Projectile Atomic Number for Z_1 -Ar	42
20	Calculated-to-Experimental Single Capture Cross Section Ratios versus Projectile Atomic Number for Z_1 -Kr	43
21	Argon K Shell Capture Cross Section Versus Proton Energy . . .	46
22	Projectile X-Ray Production Cross Section versus Projectile Energy for Fluorine on Argon	51

LIST OF TABLES

Number	Description	Page
I	Experimental and Calculated Single Capture Cross Sections for $F^{+9}, O^{+8}, N^{+7}, C^{+6}$ -Ar at Various Energies	36
II	Experimental and Calculated Single Capture Cross Sections for $F^{+9}, O^{+8}, N^{+7}, C^{+6}$ -Kr at Various Energies	37
III	Experimental and Calculated Single Capture Cross Sections for the Total and K Shell Capture and the Scaled K Shell Capture for Protons on Argon	45
IV	Table of the values used in the computer program for the evaluation of cross sections from Eq. (6) from Refs. 13 and 14	57

ACKNOWLEDGEMENTS

I wish to dedicate this work to my wife, Maureen, and to express both love and gratitude to her for her devotion. It was only through her support that this work was possible.

I would like to thank my major professor, James Macdonald, for his guidance and encouragement, not only as a teacher but also as a friend.

I extend thanks to my committee members, Carl Rosenkilde and John Eck, for their suggestions and comments concerning my work.

I am indebted to my co-workers, Louis Ellsworth, Erik Petersen, Stephen Czuchlewski, Loren Winters, and Matt Brown for their aid and willingness to give their time to me.

I would like to acknowledge James McGuire for his interest and for many helpful discussions and comments concerning the subject of this work.

I extend special thanks for the friendship and support of many people and especially to Steve Schiller, Michael Fox, Jim Johnson, Rick Workman and Tom McElroy.

I would also like to acknowledge the financial support of the U. S. Atomic Energy Commission under contract No. AT(11-1)-2130.

I. INTRODUCTION

In ion-atom collisions a number of inelastic, atomic processes may occur that have been studied in some length, both experimentally¹ and theoretically². These processes include excitation, ionization, and charge-transfer. We can assume that the magnitude of the cross section for each process depends upon the velocity of the projectile, the atomic number of both the target and projectile, the violence of the collision which may be identified by an impact parameter, the initial state of the projectile, and the final state of both projectile and target. All of these processes involve a Coulomb interaction between the projectile and target atom with a transition taking place to a different final state for at least one electron.

Consider the transition of an electron during the collision from an initial state of the target atom to some final state. If the final state of the electron is a bound state of the target the process is excitation; if the final state is a continuum state the process is ionization; while if the final state of the electron is a bound state of the projectile the process is electron capture. In all three of these processes the result of the collision is to produce a vacancy in one shell of the target atom which subsequently decays, either by emitting a photon or Auger electron, which may be detected. This paper will deal with the way in which a calculation of cross sections in a Brinkman-Kramers approximation can be used to interpret the results of a variety of experiments involving the electron capture process.

The electron capture process is a three-body problem involving the projectile ion, the target nucleus, and the target electron that is captured by the projectile. From the outset, a one-electron model is assumed to

describe the process. The electron is initially in a bound state of the target atom and after the collision is in a bound state of the projectile. The capture process is difficult to describe theoretically, even for the simplest systems, because the initial and final atomic states of the electron are not orthogonal, unless two-center molecular-like wave functions are used to describe these states dynamically. This non-orthogonality of the usual atomic basis states makes a good calculation extremely cumbersome and, even for the simplest system of protons capturing an electron from hydrogen, there is some confusion in the literature regarding which approximations give the most accurate description of the electron capture process.

For the one-electron capture process described by



the total cross section for capture from state i to f is given by,

$$\sigma_{\text{cap.}} = K \int |T_{if}|^2 d\Omega. \quad (2)$$

The constant K involves the reduced masses in the initial and final states and the relative momenta of the colliding systems. The quantities, T_{if} , are the matrix elements of the transition amplitude and, if first order perturbation theory is applied, are assumed to be replaceable by the matrix elements of the interaction potential, V_T , between the projectile and the target atom. This interaction potential can be written as the sum of two terms: (i) the interaction potential between the projectile and target nucleus, V_c , and (ii) the interaction potential between the projectile and the captured electron, V_{ep} . In other words, the interaction matrix may be written as,

$$T_{if} \approx \langle \psi_f | V_c | \psi_i \rangle + \langle \psi_f | V_{ep} | \psi_i \rangle, \quad (3)$$

where ψ_i and ψ_f are the initial and final wave functions of the system. If

ψ_i and ψ_f include orthogonal electron wave functions describing the captured electron in the two-nucleus system, then the first term above vanishes since V_c is independent of electron coordinates and ψ_i, ψ_f are orthogonal. Since the exact two-center wave functions are difficult to compute, non-orthogonal wave functions, based respectively on the target and projectile and satisfying both incoming and outgoing boundary conditions, have been used by many authors^{6,31,32} in order to approximate the capture process. It is usually assumed that both the initial and final wave functions are separable and are of the form:

$$\Psi = \psi_{\text{nucleus}} \phi_{\text{electron}} e^{i \vec{k} \cdot \vec{r}}, \quad (4)$$

where ϕ_{electron} is a hydrogenic bound state wave function.

The question now arises whether or not the projectile-nucleus term of the interaction potential, V_c , should be included in the interaction matrix, T_{if} . Several authors^{4,5} have argued that this term should be included in first order calculations to compensate for the non-orthogonality of the wave functions. Although calculations carried out in this way for protons on hydrogen show close agreement with experiment⁵, this agreement is lost as one moves to the heavy target systems since, in this case, V_c dominates the interaction and not only causes the cross section to be much larger than the experimental values, but more importantly causes the details of the electron-projectile interactions, V_{ep} , to be lost. This can be understood by observing that for $Z_2 \gg 1$, V_c dominates

$$V_T = V_{ep} + V_c = - \left(\frac{Z_1 e}{|\vec{r}|} - \frac{Z_1 Z_2 e}{|\vec{r}'|} \right), \quad (5)$$

where $Z_1 Z_2$ are the nuclear charges of the projectile and target, $|\vec{r}|$ is the

distance between the projectile and the captured electron and $|\vec{r}'|$ is the distance between the projectile and the target nucleus. Also, it can be seen, from Eq. (5), that a zero may occur in V_T and therefore the cross section that is calculated with it will pass through a minimum as the impact parameter is varied²⁴. At the impact parameter corresponding to this minimum it has been found²⁷ that higher order terms in a perturbation expansion dominate the cross section for protons on hydrogen, and hence the significance of the zero in V_T is questionable in a real capture situation. Since the V_c term does not contribute to the interaction that would be used to describe a capture-transition in an exact calculation and, since its inclusion in a perturbation-theory-calculation gives a non-physical interpretation to the problem (and the wrong results for heavy targets), it appears reasonable to omit V_c in an approximate treatment of the capture process in which trends of the cross section are to be examined. In fact, it has been shown by Bassel and Gerjuoy⁶, and Day et al.⁷ that the exclusion of the V_c term is indeed a valid approximation in the case of an infinite mass target atom. That is, for large target mass, the V_c term does not contribute to the transition probability. Therefore, a calculation which includes only the projectile-electron term in the interaction is expected to more reasonably describe the capture process.

A calculation of this type has been performed as early as 1928 by Oppenheimer⁸ and in 1930 by Brinkman and Kramers⁹. This calculation, commonly known as the Brinkman-Kramers approximation, describes the capture process for proton-like projectiles on hydrogen-like targets for ground state to ground state transitions. The cross sections obtained in this calculation are normally two to four times too large when compared with experimental

results. However, these calculations give a reasonable agreement with the experimental dependence on the velocity and final states of the electron in the projectile^{29,33}, and may give a reasonable distribution of the cross section over impact parameter.

Various authors^{10,6} have modified the Brinkman-Kramers approximation for more complicated systems using different potentials and wave functions in an attempt to take into account the non-orthogonality of the atomic basis states usually employed in the calculation. This paper will deal with a formulation in the Brinkman-Kramers approximation that was done by Nikolaev¹² and the results that can be compared to data from several different types of experiments in which the electron capture process is dominant.

Starting from the one-electron model in the Brinkman-Kramers approximation, Nikolaev, in 1967, derived a general formula of the capture cross section for arbitrary values of the external and internal screening parameters for closed shell target atoms and bare nuclei as projectiles. This approximation includes an identification of an atomic shell of equivalent electrons only by the principle quantum number n in the calculation while all information about the other quantum numbers, m and l , has been averaged for each shell. No consideration of electron spin has been made in the formulation.

The expression for the cross section for capture by a fully stripped nucleus of charge Z_1 is given by:

$$\sigma(n_1, n_2) = \pi a_o^2 \frac{2^8}{5} N_2 n_1^2 \left(\frac{v_o}{v} \right)^2 \gamma^5 \eta_n^5 (1+\beta)^{5/2} (1+\beta\gamma)^{-3} \phi_4(\beta\gamma), \quad (6)$$

where:

$$a_o = \hbar^2 / e^2 m_e, \text{ the atomic unit of length,}$$

$$v_o = e^2 / \hbar, \text{ the atomic unit of velocity,}$$

N_2 is the number of electrons in the shell from which the captured electron came in the target atom,

n_2 is the principal quantum number of the initial state of the electron in a specific target shell,

n_1 is the principal quantum number of the final state of the electron in a specific projectile shell,

u_2 is the mean velocity of the electron in the target shell,

η_n is the ratio of the electron velocity in the final to initial state: i.e. $\eta_n = Z_1 v / n_1 u_2 = (\epsilon / \epsilon_a)^{1/2}$, where $\epsilon_a = 1/2 m u_2^2$ is the binding energy of the initial state and $\epsilon = m Z_1^2 e^2 / 2 n_1^2$ is the binding energy of the hydrogen-like final state,

β gives the deviation of the target binding energy from strict hydrogen-like scaling: $\beta = \left(\frac{Z_2^*}{n_2^*} \right)^2 \left(\frac{13.6}{\epsilon_a} \right) - 1$,

$\gamma = 4(1+2(1+\eta_n)V^{-2} + (1-\eta_n^2)V^{-4})^{-1} V^{-2}$, and

V is the ratio of the projectile velocity to the velocity of the electron in the target: v/u_2

$$\phi_4(\beta\gamma) = \begin{cases} (1-.25\beta\gamma) & \beta\gamma \leq 1 \\ (1+\beta\gamma)^{-.46} & \beta\gamma < 5. \end{cases}$$

The binding energies used for specific target shells are taken from Lotz¹³ and the screened nuclear charge values from Clementi and Raimondi¹⁴.

In deriving Eq. (6), Nikolaev has introduced the important external screening parameter, β . However, if no screening is included (i.e. $\beta=0$),

Eq. (6) reduces to

$$\sigma(n_1, n_2) = \pi a_o^2 \frac{2^8}{5} N_2 n_1^2 \left(\frac{v_o}{v} \right)^2 \gamma^5 \eta_n^5, \quad (7)$$

or

$$\sigma(n_1, n_2) = \pi a_o^2 \frac{2^{18}}{5} \frac{u_2^5}{v^{12}} \frac{Z_1^5 v_o^7 N_2}{n_1^3} \left[\frac{1}{(1+2(1+\eta_n)V^{-2} + (1-\eta_n^2)V^{-4})} \right]^5, \quad (8)$$

or

$$\sigma(n_1, n_2) = \frac{\pi a_o^2 2^{18} (Z_1 Z_2)^5 v_o^{12} N_2}{5 n_2^5 n_1^3 v^{12} [(1+2(1+\eta_n)V^{-2} + (1-\eta_n^2)V^{-4})]^5}, \quad (9)$$

which can be shown to be equivalent to the expression for the capture cross section derived by Schiff²⁴ and others^{9,25,3}. In the limit of high projectile velocity, v , this reduces further to the more familiar form

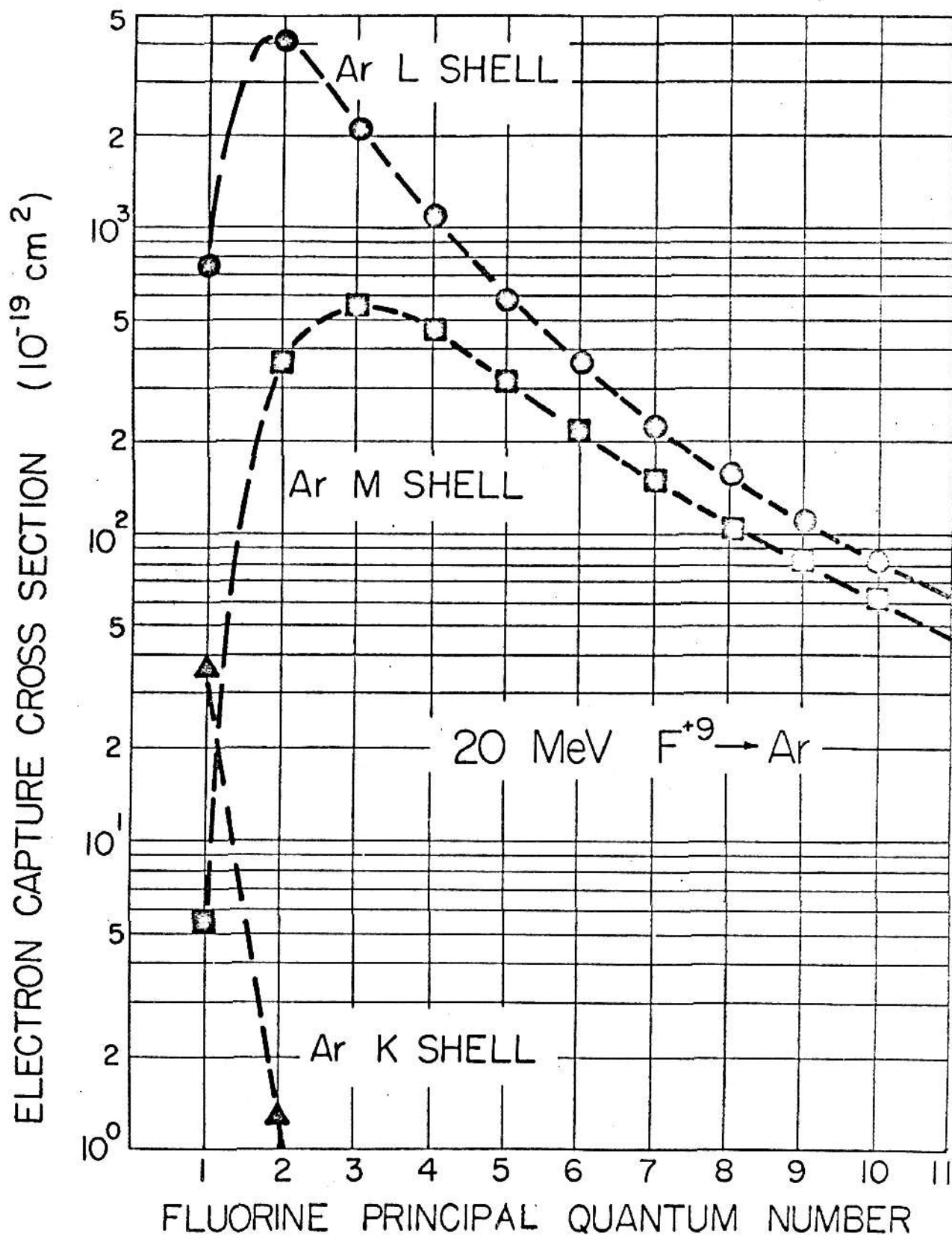
$$\sigma(n_1, n_2) = \frac{\pi a_0^2 2^{18} N_2 (Z_1 Z_2)^5}{5 n_2^5 n_1^3 v^{12}}, \quad (10)$$

which is independent of the velocity ratio of the final to initial states, η_n . This parameter becomes important at low projectile velocities since the scaled projectile velocity, V , is then small enough to allow η_n to contribute to the cross section. In this velocity range, η_n is large for low binding energy target electrons and heavy projectiles. Thus, the inclusion of this parameter decreases the cross sections. For example, fluorine ions with hydrogen-like binding energies of 1100, 275, and 122 eV for the K, L, and M shells respectively, incident on hydrogen atoms with 13.6 eV binding energy electrons have values for η_n of 81, 21, and 9 which are particularly important for $V < 5$. On the other hand, if the target and projectile are both heavy the capture cross section obtained in Eq. (6) reflects the level matching effects and will contain a maximum for $\eta_n \approx 1$. A typical maximum for heavy ions is shown in Fig. 1. It can be seen that for 20 MeV fluorine on argon a maximum occurs in the capture cross section from the L shell of argon (270 eV) to the $n_1 = 2$ shell (275 eV) of the fluorine ion. Finally, for high n_1 states, η_n is small enough to be neglected and the cross section then falls as $1/n_1^3$ as in the high velocity limit.

The closed form of Eq. (6) was obtained by assuming that the target shells are completely filled, and therefore, it is understood that all target shells will be approximated as completely closed to avoid the cumbersome expression that would result otherwise¹². In the cases examined in this

**THIS BOOK
CONTAINS
NUMEROUS PAGES
WITH DIAGRAMS
THAT ARE CROOKED
COMPARED TO THE
REST OF THE
INFORMATION ON
THE PAGE.**

**THIS IS AS
RECEIVED FROM
CUSTOMER.**



Calculated electron capture cross section versus the fluorine principal quantum number for $20 \text{ MeV } \text{F}^{+9} \rightarrow \text{Ar}$.

work this is a good approximation for all but the outermost shells which are relatively unimportant in the energy range of the experiments discussed. It should be noted that the calculation gives the cross section in units of cm^2/atom and since some targets exist as molecules, such as H_2 or N_2 , Eq. (6) has been multiplied by a factor of two, under the assumption that the atoms of the molecules interact independently. This is a good assumption at projectile velocities higher than in molecular orbitals and because capture cross sections are smaller than geometric areas of the atom. In terms of absolute values it will be shown that Eq. (6) does not agree with experimental values. However, when it is used to compare relative contributions of the capture cross section or when it is normalized to experimental values, Eq. (6) can be very useful in determining trends in the electron capture cross section.

It is known³, that the Brinkman-Kramers approximation gives values that are approximately three times too large for protons. Therefore, over the energy range of .02-.5 MeV Nikolaev has made a fit of these calculated cross sections to the experimental values for protons capturing electrons from a number of targets to obtain the empirical fitting function:

$$R_o(t) = .3 \left((7t/9)^{-8} + 7t/9 \right)^{-2}, \quad (11)$$

where:

$$t = v/v_o \sqrt{b_a} \quad (12)$$

$$b_a = Z_2^2/n_2^2 \text{ of the specific shell of the electron captured from the target atom.} \quad (13)$$

Then, the total capture cross section is given by

$$\begin{aligned} \sigma_{\text{cap. total}} = & R_o(\text{Kshell}) \sigma(n,1) + R_o(\text{L shell}) \sigma(n,2) + \\ & R_o(\text{M shell}) \sigma(n,3) + \dots \end{aligned} \quad (14)$$

This function, $R_o(t)$, although fitted using cross sections for low proton energies seems to have the correct form for higher velocity protons

as well²². However, it does not represent a universal function for all projectile-target systems, and one would expect a dependence of $R_o(t)$ on Z_1 and n_1 if one were to form a universal fitting function. For heavy projectiles the calculated capture cross sections given by Eq. (6) become increasingly larger than the experimental values as the projectile nuclear charge increases. This increase is not taken into account in the fitting function, $R_o(t)$, and therefore its inclusion, in Eq. (9) for the total capture cross section is not strong enough to lower the calculated cross sections to the experimental values.

Equation (6) is used in this paper to calculate partial and total capture cross sections that are compared to the results of several different experiments in which charge exchange is expected to be a dominant collision process. To facilitate the computation of cross sections using this Brinkman-Kramers formulation, the computer program listed in the appendix was used to produce $\sigma(n_1, n_2)$ for all the target electrons captured to all shells. No attempt is made to find a universal function to reduce the calculated cross sections to give agreement with the absolute value of experimental cross sections. Hence, only the trends of the capture cross section are being examined in this work.

II. ELECTRON CAPTURE EXPERIMENTS

A. Total Capture for Protons

The Brinkman-Kramers formulation has been used previously to compare experimental total capture cross sections for protons in various gasses in the energy range below 500 keV. The fitting function, R_0 , discussed previously, was determined to account for the overestimate inherent in Eq. (6). Since the capture of more tightly bound electrons becomes increasingly more important at higher velocities, an important comparison of the results of Eq. (6) with proton electron capture cross sections at higher velocities can be made.

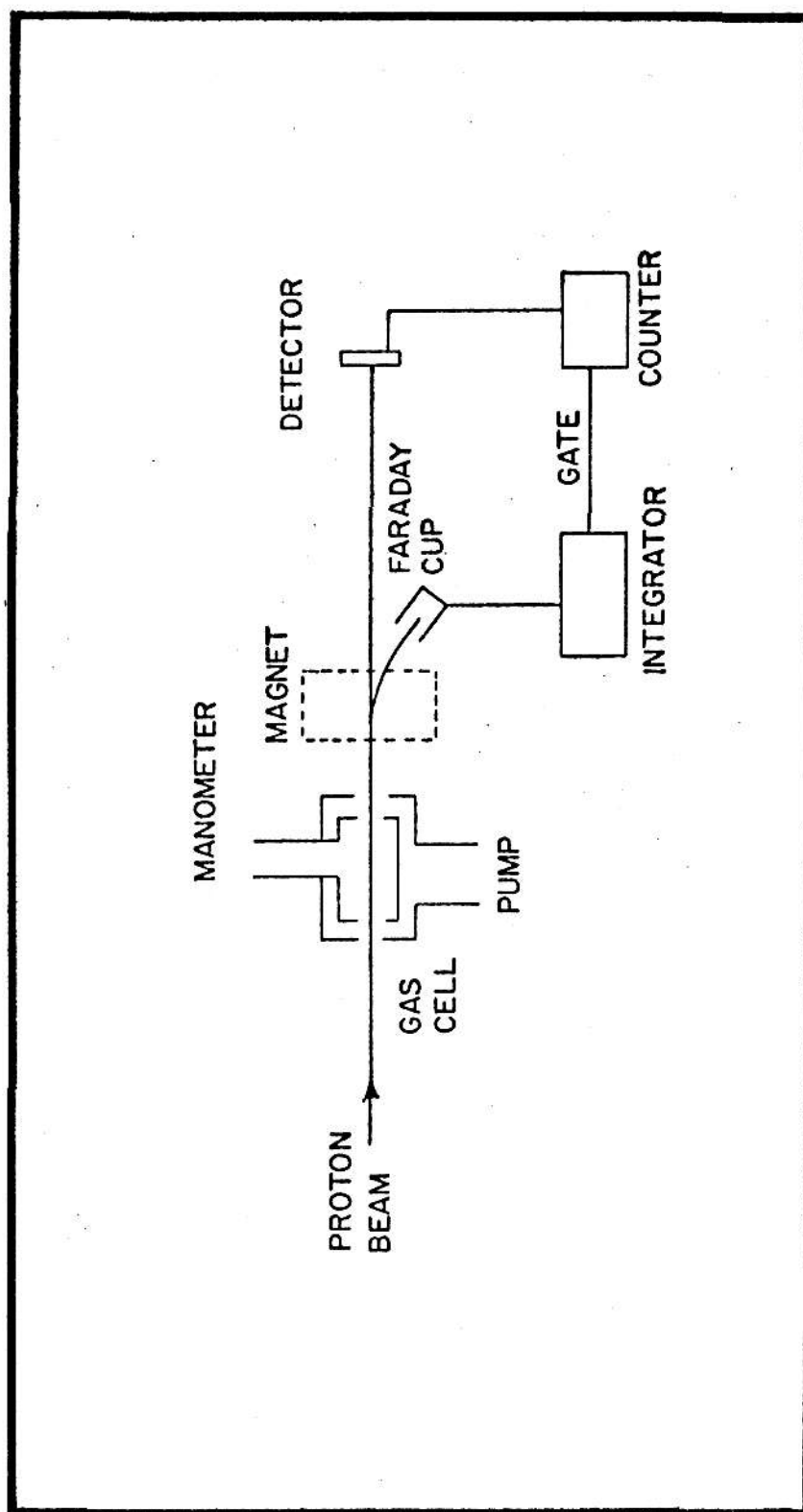
In this type of experiment energetic protons are incident on a gas target and, with a small cross section, capture electrons into a particular shell in large impact parameter collisions. Figure 2 shows a schematic of the experimental arrangement. The neutral hydrogen atoms are not deflected by the magnetic field but the proton beam is deflected into the large, suppressed Faraday cup in which the current is measured. The neutral atoms are detected by a single particle surface barrier detector which allows individual atoms to be detected in the presence of a large proton current.

In this experiment the number of neutrals, N_0 , the pressure in the gas cell and the number of protons are measured. The total number of particles, N_T , in the beam is essentially the same as the number of protons and, therefore, the expression for the cross section for the electron capture process is given by:

$$\sigma_{10} = \frac{d\mathcal{P}_0}{d\pi}, \quad (15)$$

where \mathcal{P}_0 is the fraction of neutral particles to the total number of particles,

FIGURE 2



Schematic of the apparatus for the determination of total electron capture yields for protons in gases.

N_o/N_p , and π is the target thickness which is related to the pressure by

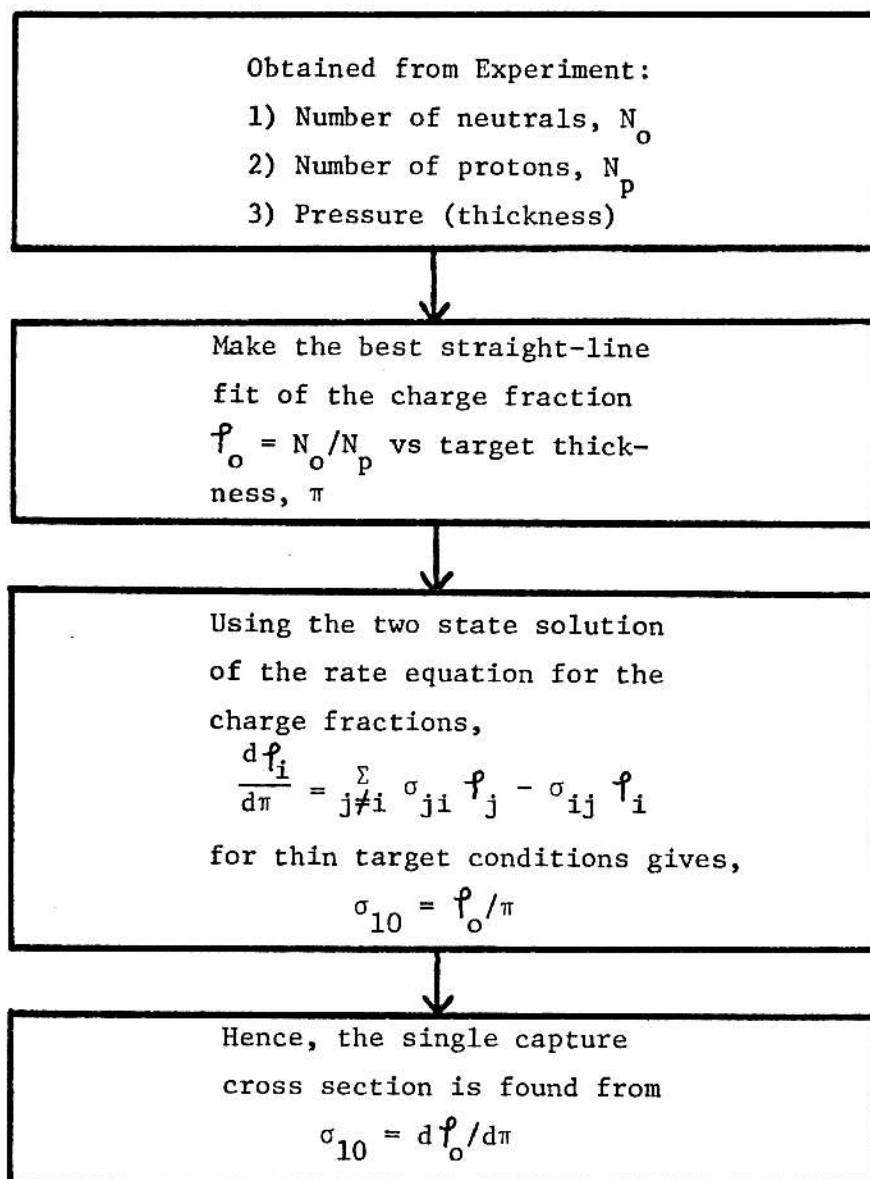
$$\pi = \frac{N_o P l}{RT} , \quad (16)$$

where N_o is Advogadro's number, l is the length of the gas cell, P is the pressure in the gas cell, R is the gas constant, and T is the temperature (See Fig. 3).

No information is obtained in this experiment regarding the shell from which the electron came, nor the shell of the projectile into which it was captured; it is only known that the electron was, in fact, captured from the target. Hence, the relevant cross section for comparison with the theory is the total capture cross section of Eq. (6) given by

$$\sum_{n_1, n_2} \sigma(n_1, n_2) .$$

FIGURE 3



Flow chart for the analysis of the single capture cross section for protons, σ_{10} .

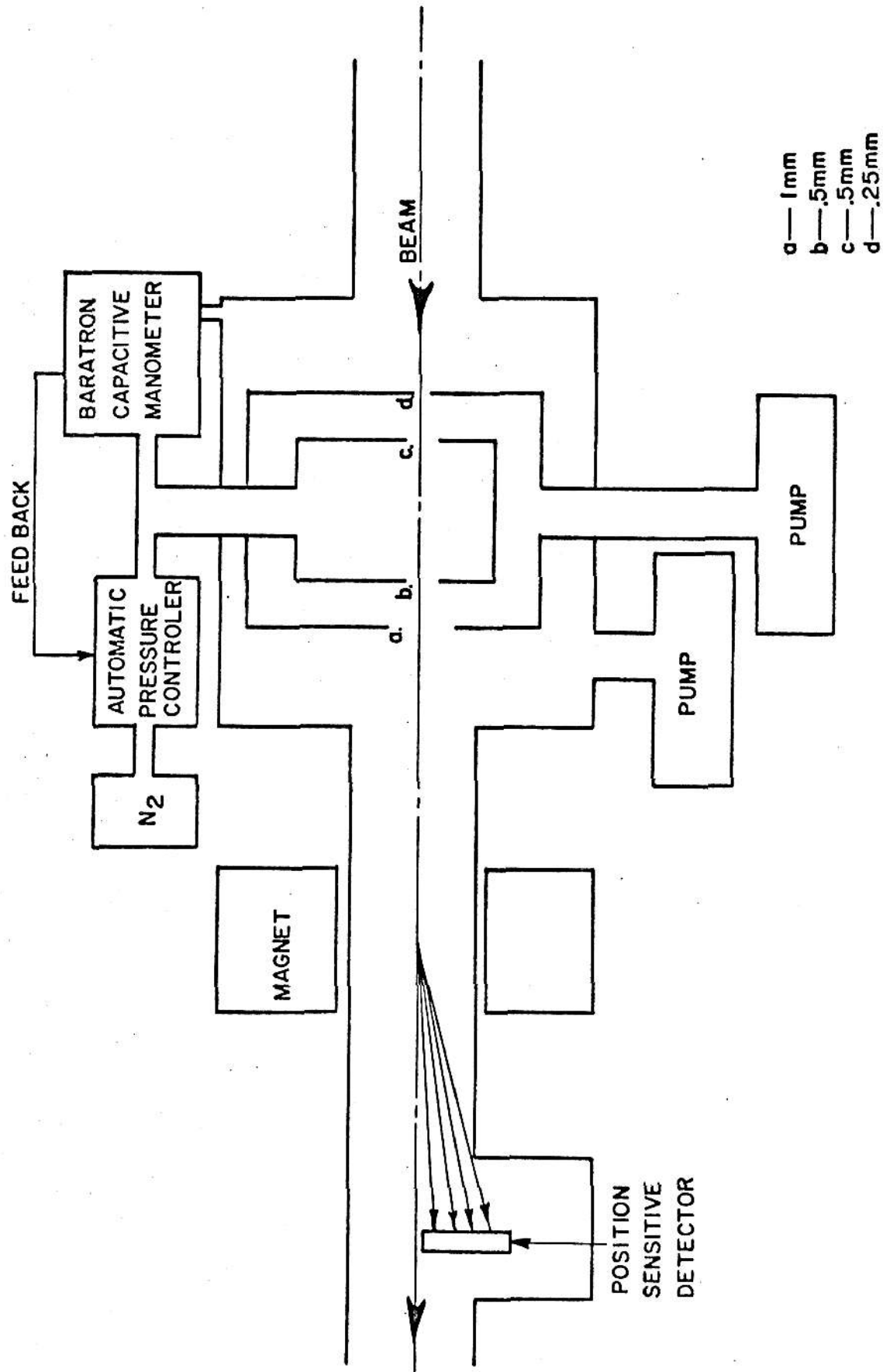
B. Total Single Capture for Heavy Bare Projectiles

When protons are used as the projectile in atomic collisions, the fraction of the incident beam that undergoes electron capture is small. On the other hand, if heavy projectiles are used the capture cross sections are several orders of magnitude higher at the same velocity. Hence, the capture process may make a significant contribution to the vacancy production¹⁹ of the target atom in addition to the vacancies produced by the ionization process.²⁸ To consider the validity of estimates of the importance of capture events, it is of interest to compare the results of Eq. (6) with the total single electron capture cross section obtained experimentally.

In these experiments heavy projectiles are incident on gas targets and capture one or more electrons in a single collision. The experimental arrangement that has been used for these experiments is shown in Fig. 4. After traversing the gas cell, the beam passes through a magnet which separates it into its different charge states. A position sensitive detector is used to detect the ions of all different charge states emerging from the gas cell.

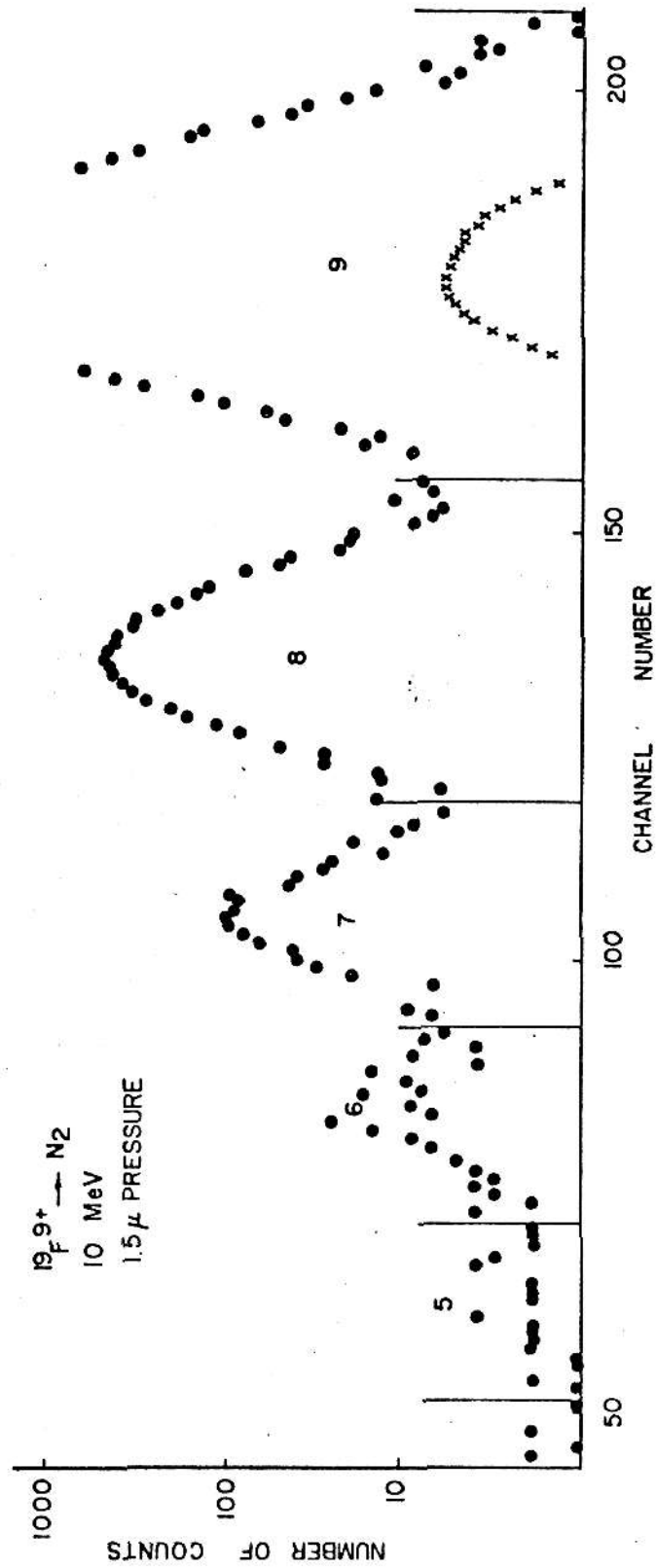
A typical charge state spectrum of the data obtained in this type of experiment is given in Fig. 5 for $F \rightarrow N_2$ ¹⁵. It consists of several peaks which represent the number, N_i , of particles in each charge state after the beam has passed through the gas cell. The charge fractions, P_i , can then be determined, where $P_i = N_i / \sum_j N_j$. From a measurement of the pressure dependence of P_i and a knowledge of the initial charge state of the projectile, a first order approximation to the cross sections, $\sigma_{\alpha i}$, (from charge state α to charge state i) can be obtained by using the "growth of charge state method",¹⁷ (See Fig. 6). By using all incident charge states, α , a complete first order set

FIGURE 4



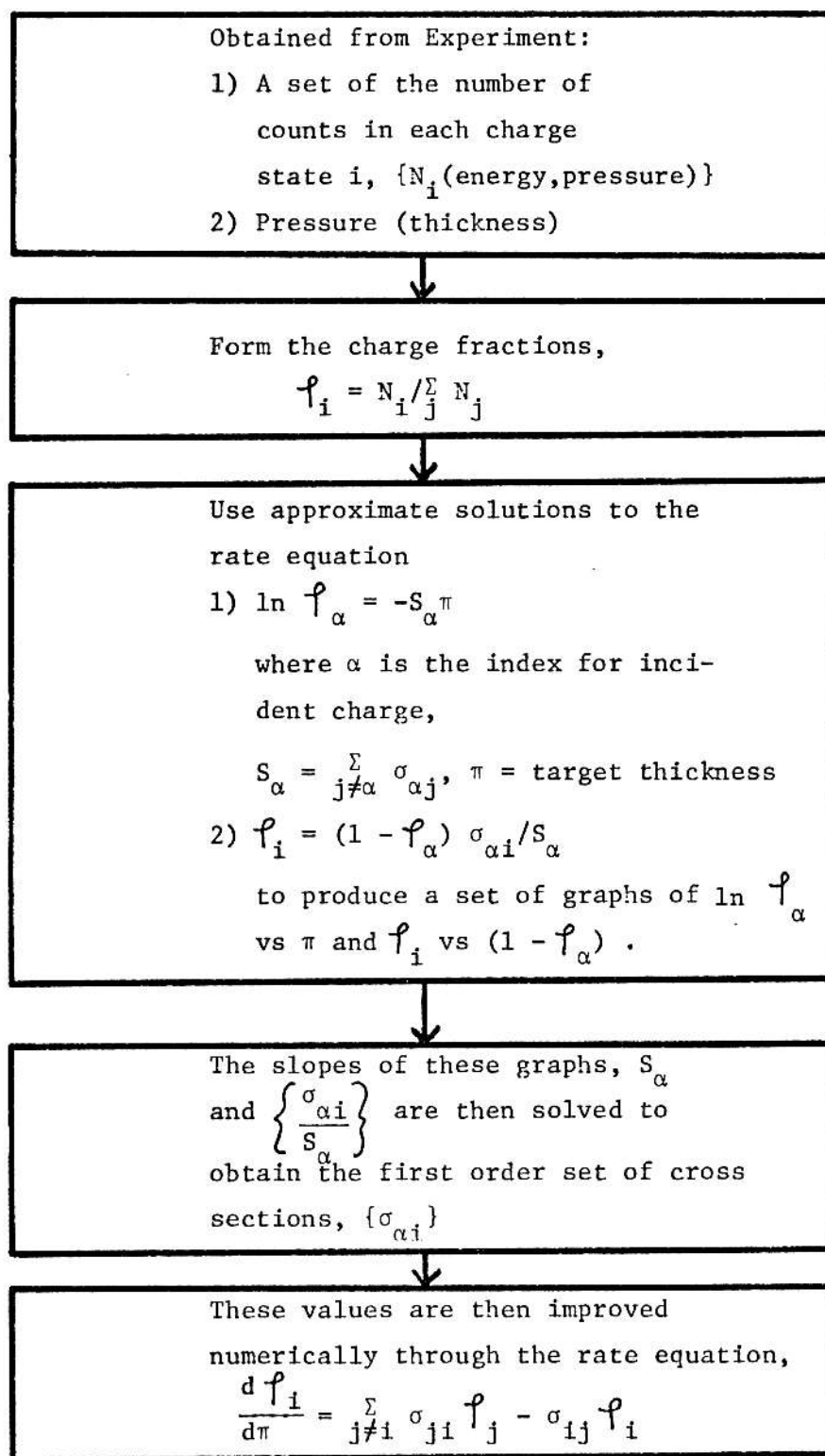
Schematic diagram of the apparatus for the determination of electron capture yields for heavy bare projectiles.

FIGURE 5



Typical spectrum of particle detector counts versus channel number for a heavy ion charge exchange experiment. In this case, the system is 10 MeV fluorine on nitrogen.

FIGURE 6



Flow chart for the analysis of the electron capture cross sections, $\sigma_{\alpha i}$, (from charge state, α , to charge state, i) in heavy projectile systems.

of charge exchange cross sections is obtained which can be used to integrate the differential equations governing the growth and decay of each charge state and, at each value of target thickness used in the experiment, the populations in each charge state can be calculated. These values are then compared with the corresponding experimental data, the sum of the squares of the deviations are determined and minimized using an iteration process to modify the set of cross sections. Agreement is reached within the statistics of the experiment after several iterations and the corrected set of cross sections, with probable errors commensurate with the least squares sums, are calculated.

Again, no information about particular shells of the target or projectile is obtained and, therefore, the relevant comparison with the theory is for the total capture cross section,

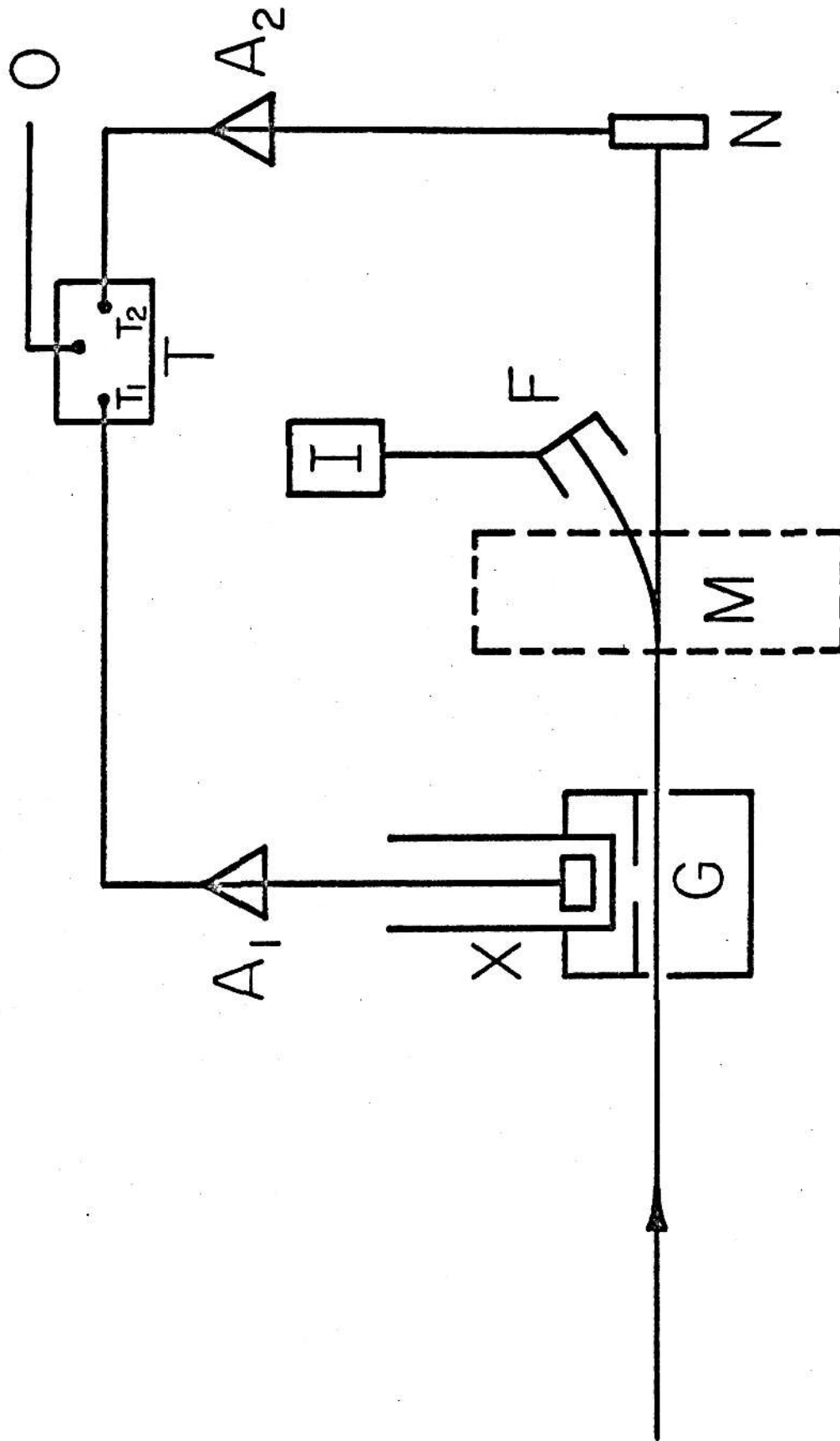
$$\sum_{n_1, n_2} \sigma(n_1, n_2) .$$

C. Capture From a Particular Shell of the Target by Protons

As mentioned previously, the capture process may contribute significantly to the target inner shell vacancy production cross section. For heavy projectiles the capture cross sections may be comparable in magnitude to the ionization cross section. Therefore, experiments, which give information about the relative role of the capture process in inner shell vacancy production, as well as a reasonable theoretical explanation are important. In view of this, it is of interest to compare the relevant sum of the capture cross sections given by Eq. (6) with experimental values of inner shell capture cross sections by protons.

In this type of experiment a coincidence technique is used in order to gain information about the cross section for the capture process from a particular shell of the target to protons, (See Fig. 7)¹⁸. If the proton captures an electron from the target in the collision it is subsequently detected in a neutral particle detector. If the capture was from the K shell of the target, then a K shell x-ray will occur for a certain fraction of the vacancies produced and may be detected in a Si(Li) detector. The output of these two detectors can be used as stop and start signals respectively for a time-to-amplitude converter (TAC). The output of the TAC will represent delayed coincidences between target K shell x ray emission and projectile electron capture. The output of both detectors is monitored separately in addition to the coincidences, so that the total capture cross section by the incident proton beam is obtained. The emerging proton beam is deflected magnetically into a Faraday cup for normalization purposes.

FIGURE 7



Schematic diagram of the apparatus for the determination of the coincidences between electron capture from the K shell of a gas target by protons. The lettered components are the gas cell (G), the magnet (M), Faraday cup (F), integrator (I), surface barrier detector (N), Si(Li) detector (X), amplifiers (A), and time-to-amplitude converter (T).

The particular system that has been investigated is the capture of K shell electrons of Ar by protons¹⁸. The experiment allowed the measurement of the total number of neutral atoms, N, the total number of Ar K x-rays, X, the number of real coincidences, C, the pressure, and the number of transmitted protons.

The number C/K gives the ratio of coincidence counts divided by the number of K shell x-rays and is equal to $\frac{\sigma_{CK}}{\sigma_{VK}}$, where σ_{CK} is the capture cross section from the argon K shell and σ_{VK} is the vacancy production cross section of the argon K shell. The ratio C/N gives the number of coincidence counts observed divided by the total number of capture events. Since this involves two different detectors, the efficiency ϵ_x and fluorescence yield w_x must be taken into account to relate this to cross sections so that

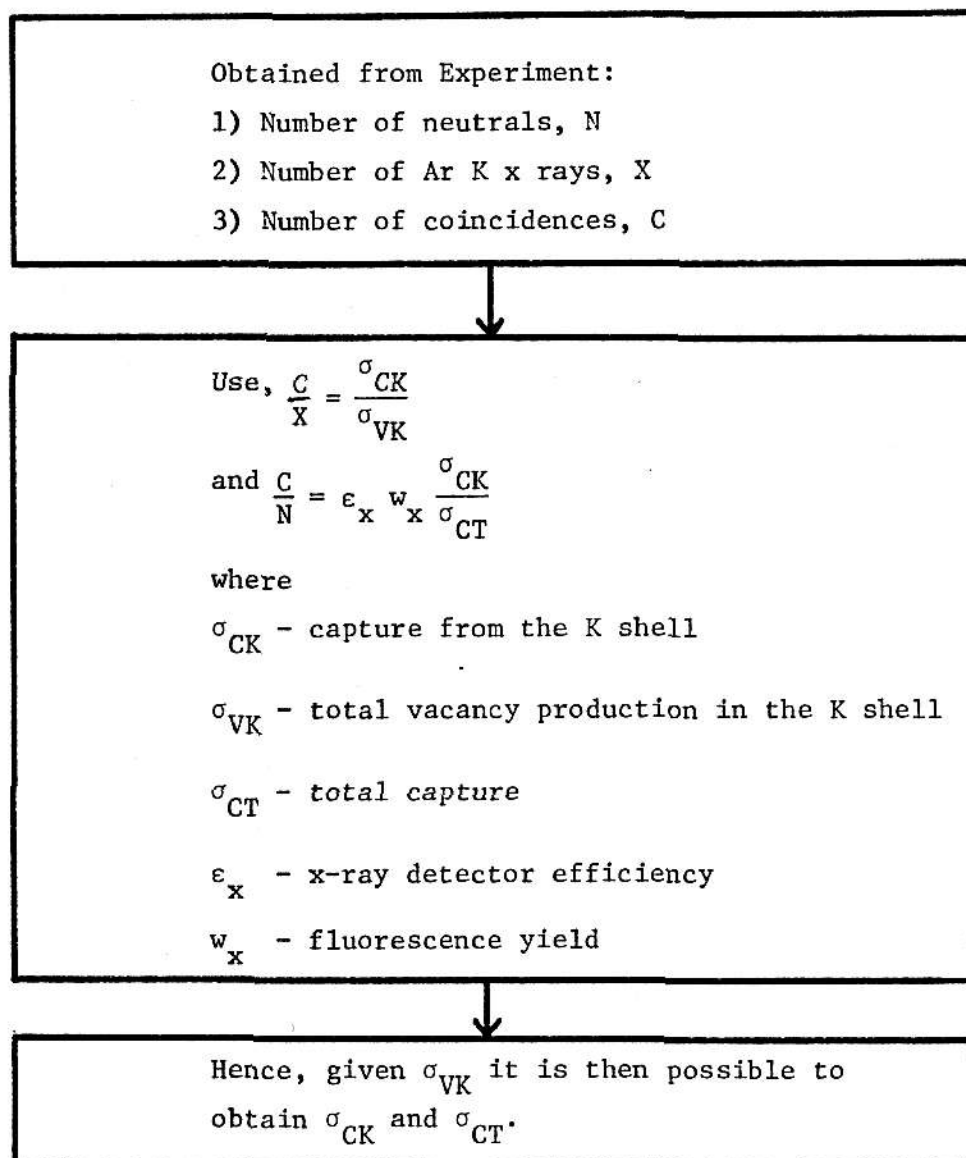
$$\frac{C}{N} = \epsilon_x w_x \frac{\sigma_{CK}}{\sigma_{CT}}, \quad (17)$$

where σ_{CT} is the total capture cross section from all shells of the target. Using this information, along with the previously measured values¹⁹ for the K shell vacancy production cross section, σ_{VK} , the total capture cross sections discussed previously in section IIA, as well as the cross sections for capture from the K shell of Ar, were obtained (See Fig. 8).

The analysis of the experiment gives the cross section for the capture of an electron from the K shell of the argon atom to any shell of the proton and, therefore, the relevant values of the theory to compare to this experiment are given by

$$\sum_{n_1} \sigma(n_1, n_2) ; n_2 = 1 .$$

FIGURE 8



Flow chart for the analysis of the total single capture cross section, σ_{CT} , and the cross section for capture from the K shell of the target, σ_{CK} .

D. Capture to a Particular Shell(s) of the Projectile

The theoretical values given by Eq. (6) for the capture cross section are for the capture of an electron from a particular shell, n_2 , of the target, to a particular shell, n_1 , of the projectile. For protons the capture to excited states varies approximately as $(1/n_1^3)$; however, for heavy projectiles this dependence does not hold. In order to test the calculated dependence of capture to excited states of the projectile a comparison of the calculated values to values obtained in experiments involving projectile x-rays has been performed.

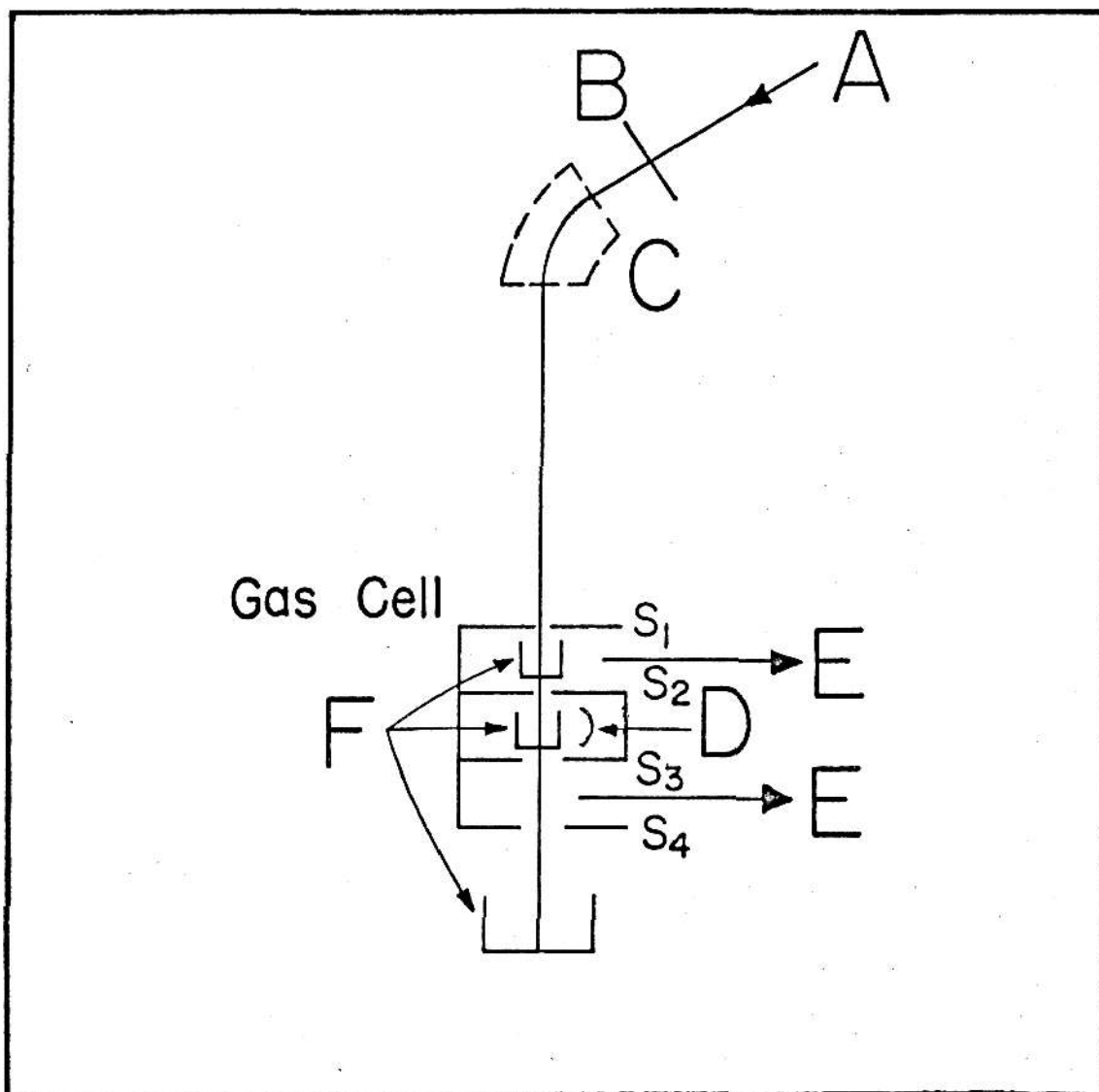
In this type of experiment the projectile, rather than the target, is observed, under single collision conditions with gas targets (See Fig. 9). If the projectile is bare as it approaches the target atom and later emits an x ray, then it must have captured an electron or electrons into a shell with $n_1 \geq 2$. Following cascading, x-ray emission from p states can be observed. This radiation is assumed to be isotropic³⁵ and x-ray production cross sections are determined.

One system that has been examined is the reaction $F^{+9} \rightarrow Ar$ studied by Brown²⁰ et al. In this experiment the number of F K shell x-rays were counted and this yield is measured as a function of pressure for fixed energy. From the measurement it was possible (See Fig. 10) to arrive at the cross section for K shell x ray production for the F ion using,

$$\sigma_x = K \frac{\Delta Y}{\Delta P} \frac{\text{cm}^2}{\text{atom}}, \quad (18)$$

where Y is the x ray yield, P is the pressure, and the constant, K, involves the number of incident particles, geometric factors, and detector efficiency. The x-ray cross section corresponds to a fraction of the cross section for

FIGURE 9



Schematic diagram of the apparatus for the determination of projectile x-ray yields in gases. The lettered components are the ion beam (A), stripping foil (B), analysing magnet (C), proportional detector (D), pumping outlets (E), Faraday cups (F), apertures (S).

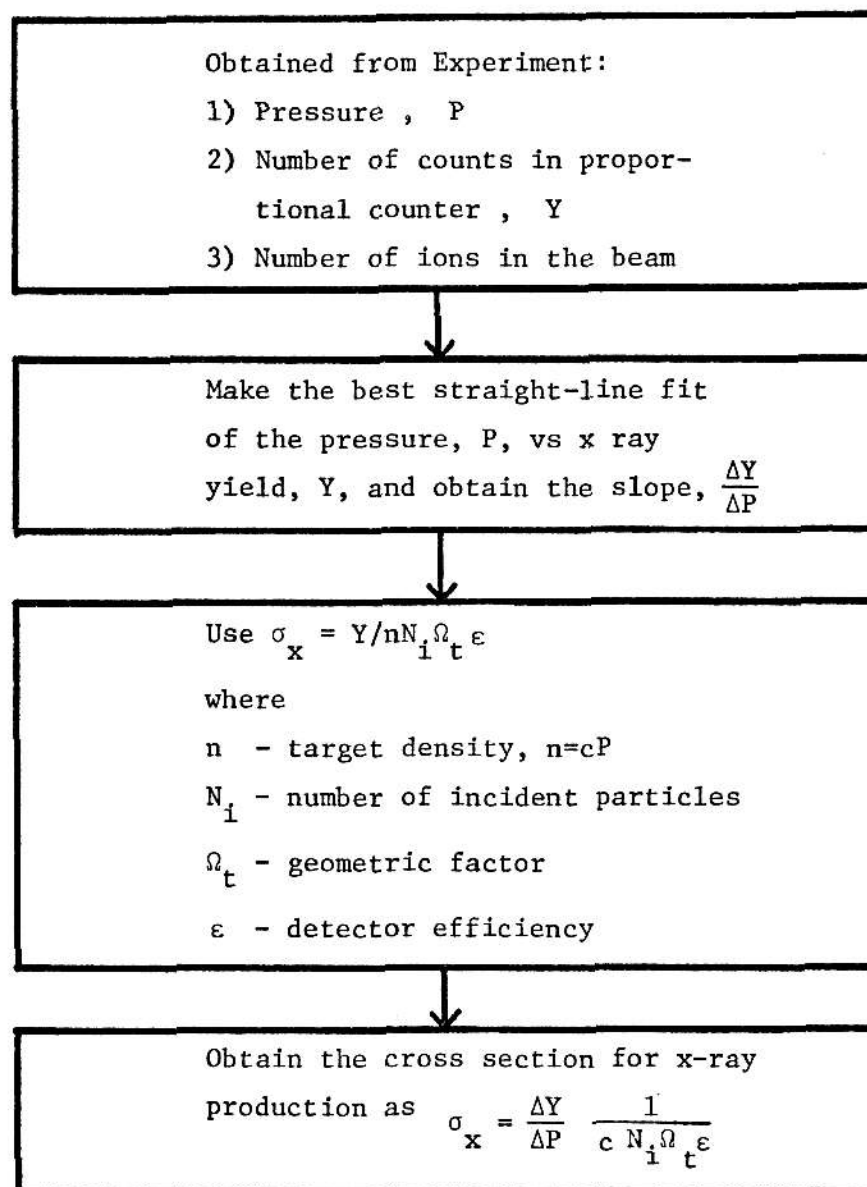
the capture of an electron to all excited states of the projectile that decay through p states.

As will be discussed in section IIID not all of the capture events leading to excited states of the fluorine ion will result in an observable K shell x ray and, therefore, the relevant values to compare to this experiment from Eq. (6) are given by some fraction of those capture events into $n_1 = 2$, plus some other fraction of those capture events into $n_1 > 2$.

$$1/A \sum_{n_1=2, n_2} \sigma(n_1, n_2) + 1/B \sum_{n_1>2, n_2} \sigma(n_1, n_2) ,$$

where $1/A$ and $1/B$ are the fractions of capture events which result in a F K shell x ray.

FIGURE 10



Flow chart for the analysis of the cross section for x-ray production, σ_x .

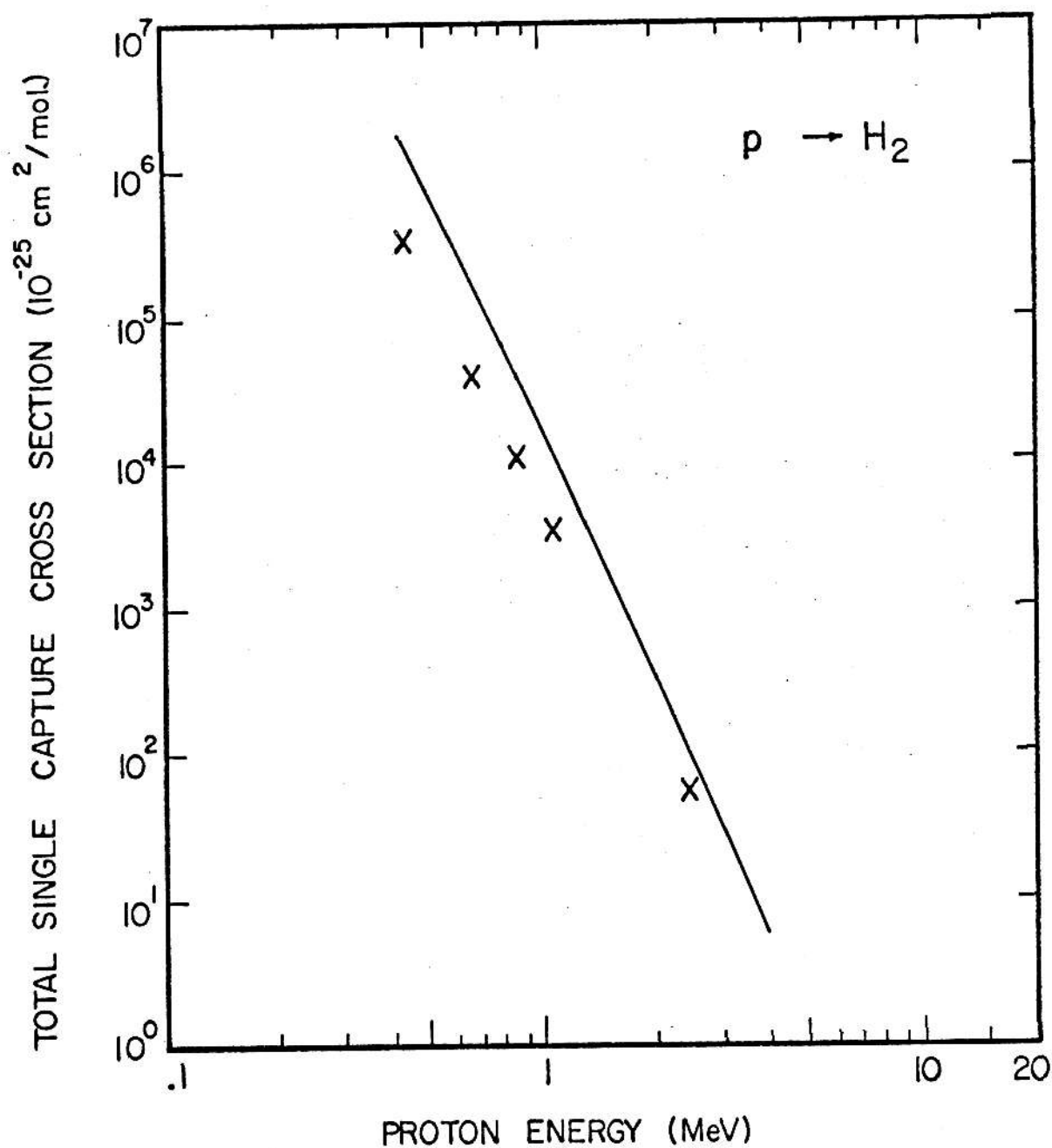
III. COMPARISON OF CALCULATION TO EXPERIMENTAL RESULTS

A. Total Capture for Protons

In the past there have been a number of investigations of the electron capture by proton beams of various energies on a variety of targets²³. The experiments used for this comparison with the results of Eq. (6) are those of Welsh et al.²¹ for protons in H_2 , He, N_2 , and Ar. The experimental values for the total capture cross sections were obtained as described in section IIA and are shown in Fig. 11-15 along with the calculated cross sections given by Eq. (6). In all cases the calculated values are larger than the experimental values by approximately a factor of four. However, the calculated values do give the correct energy dependence over the range indicated. It should be pointed out that the experiment for hydrogen and nitrogen were performed using the molecules H_2 and N_2 and, therefore, the calculated values of Eq. (6) have been multiplied by 2 in order to take this into account assuming that the atoms of the molecules interact independently.

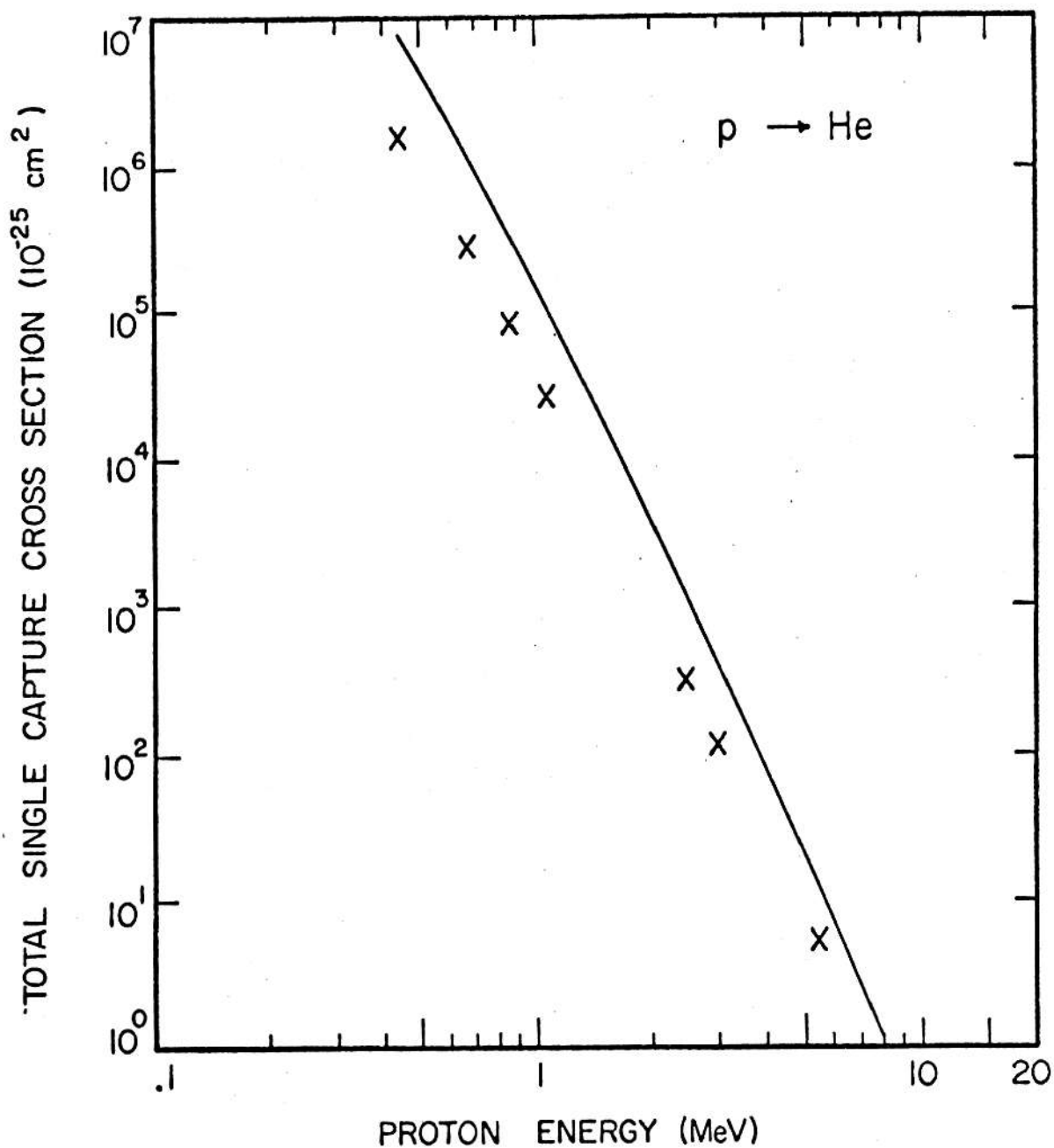
The ratios obtained by comparing the calculated value to the experimental value for the capture cross section can be used as a normalization factor for other predictions that can be obtained from Eq. (6) for capture processes involving protons. This will be discussed in section IIIC. Nikolaev has made the comparison between experimental total capture cross sections and this Brinkman-Kramers formulation and he has found a "universal" empirical fitting function that gives agreement to $\pm 20\%$. This fitting function is given by Eq. (8), but has no dependence on projectile atomic number that would provide a scaling to other hydrogen-like ions. For protons, the form of the fitting function (Eq. (8)) extrapolated from the low energy range, in which the empi-

FIGURE 11



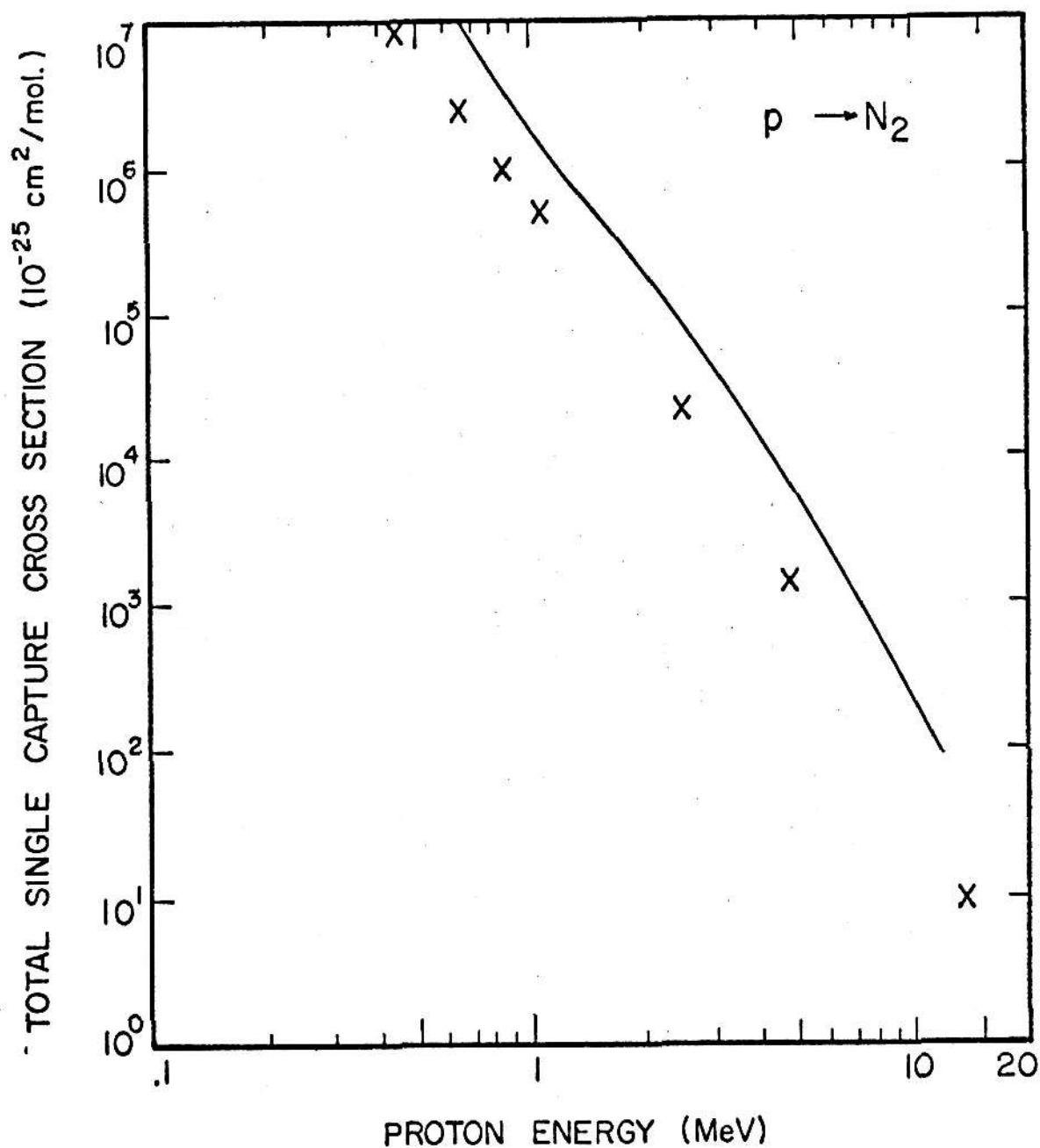
Total single capture cross section versus proton energy for protons on hydrogen. The experimental values from Ref. 21 are represented by the X's, while the calculated values from Eq. (6) are given by the solid line.

FIGURE 12



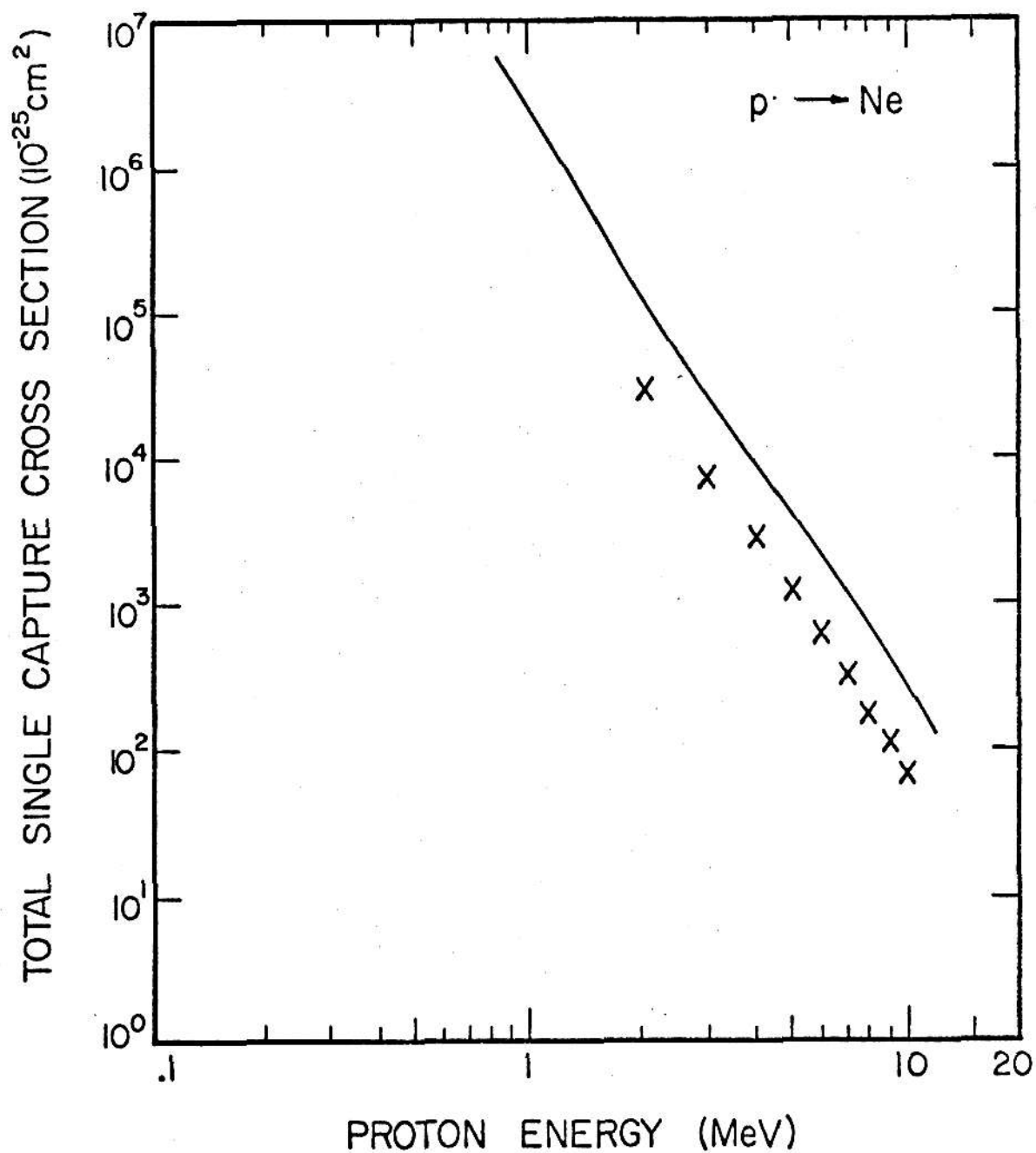
Total single capture cross section versus proton energy for protons on helium. The experimental values from Ref. 21 are represented by the X's, while the calculated values from Eq. (6) are given by the solid line.

FIGURE 13



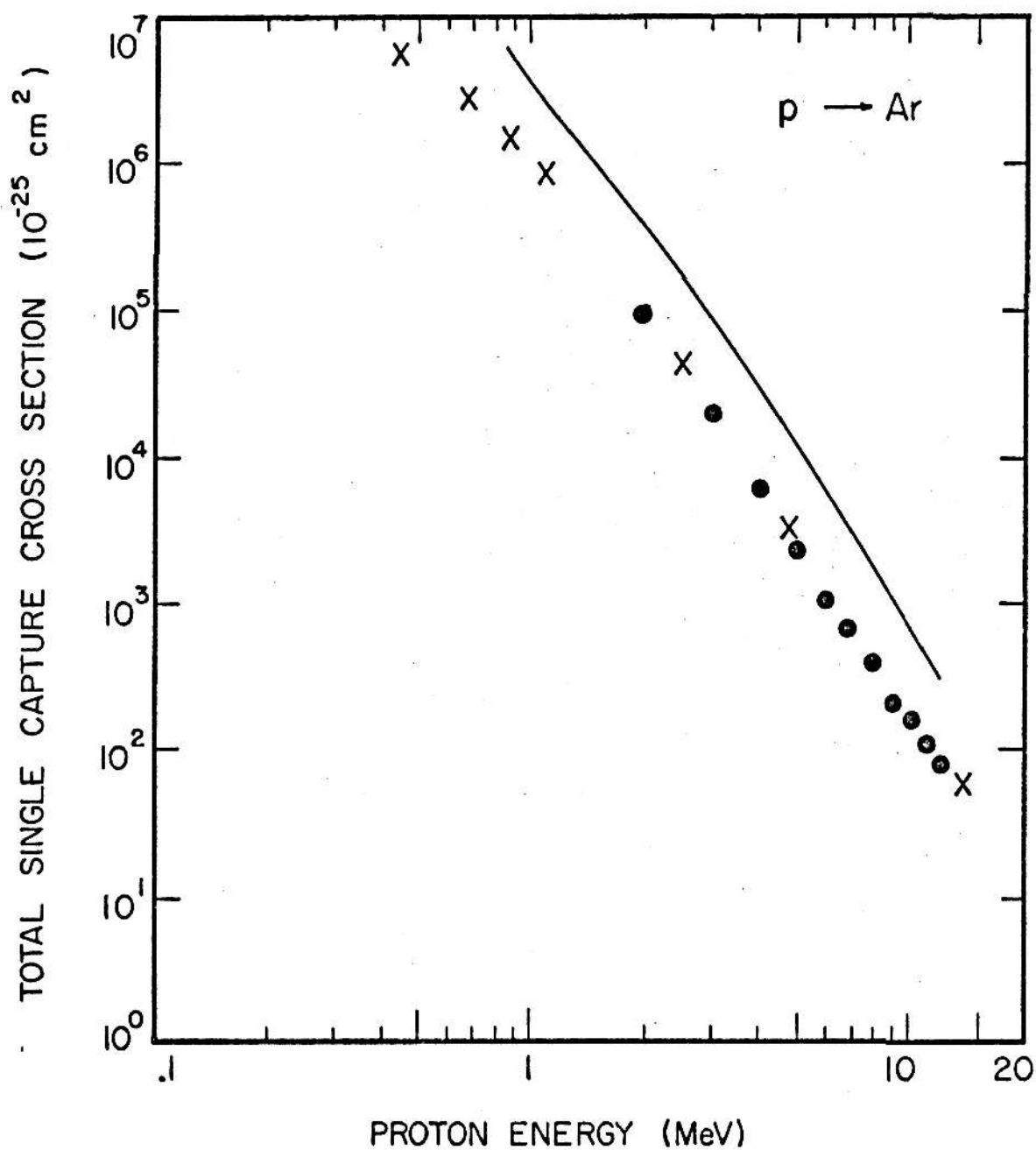
Total single capture cross section versus proton energy for protons on nitrogen. The experimental values from Ref. 21 are represented by the X's, while the calculated values from Eq. (6) are given by the solid line.

FIGURE 14



Total single capture cross section versus proton energy for protons on neon. The experimental values from Ref. 21 are represented by the X's, while the calculated values from Eq. (6) are given by the solid line.

FIGURE 15



Total single capture cross section versus proton energy for protons on argon. The experimental values from Ref. 21 are represented by the X's and those from Ref. 19 are represented by the •'s, while the calculated values from Eq. (6) are given by the solid line.

rical fit was made¹², to the higher energy range of the experiments by Welsh et al.²¹, results in cross sections which are within the $\pm 20\%$ agreement claimed.

B. Total Single Capture for Heavy Bare Projectiles

Experiments in which electron capture by bare heavy ions are measured have been carried out in a number of investigations in the past^{11,17,30}. For the comparison with the cross sections calculated in the Brinkman-Kramers formulation, experimental results of Chiao¹⁵ for F^{+9} , C^{+6} , N^{+7} on Ar and Kr, and of Macdonald and Martin for O^{+} on Ar¹⁶ were used. The analysis of these charge transfer reactions was performed as stated in section IIB to obtain the single capture cross sections. Although this analysis gives the experimental cross sections for multiple capture in a single collision as well as single capture, only the single capture cross sections are relevant to compare to the calculated cross sections. These single capture cross sections have been plotted as a function of the incident energy of the projectile, and from a smooth curve drawn through these points, values for the cross sections have been obtained for comparison with the calculated values obtained by using Eq. (6). Both sets of results are listed in Tables I and II for the various reactions and a typical plot of these values is given for F^{+9} on Ar in Fig. 16. It is obvious from the figure that the calculation grossly overestimates the cross section. To emphasize this overestimate, the ratios of the calculated to the experimental capture cross section (tabulated in Tables I and II) are plotted in Figures 17 and 18 for targets of Ar and Kr and are seen to fall with increasing incident energy for each projectile. This implies that the calculation may be better at higher energies, although in all cases the calculated value is approximately an order of magnitude too large even at the highest energy used. These same ratios are plotted against projectile atomic number, Z_1 in Figures 19 and 20. If we assume that the oxygen data is about

TABLE I

Projectile	<u>F⁺⁹, O⁺⁸, N⁺⁷, C⁺⁶, → Ar</u>			
	Energy(MeV)	$\sigma_{\text{exp.}} (10^{-16})$	$\sigma_{\text{calc.}} (10^{-16})$	$\frac{\sigma_{\text{calc.}}}{\sigma_{\text{exp.}}}$
F ⁺⁹	10	1.51	62.51	41.39
	15	.81	23.87	29.46
	20	.53	11.97	22.58
	25	.42	6.99	16.64
O ⁺⁸	10	.60	29.15	48.4
	15	.32	11.25	35.2
	20	.23	5.69	24.7
	25	.18	3.30	18.4
N ⁺⁷	10	.51	14.78	28.98
	15	.34	5.80	17.05
	20	.22	2.93	13.0
	25	.14	1.66	11.71
C ⁺⁶	10	.309	7.099	22.97
	15	.212	2.739	12.91
	20	.147	1.332	9.061
	25	.101	.7254	7.182

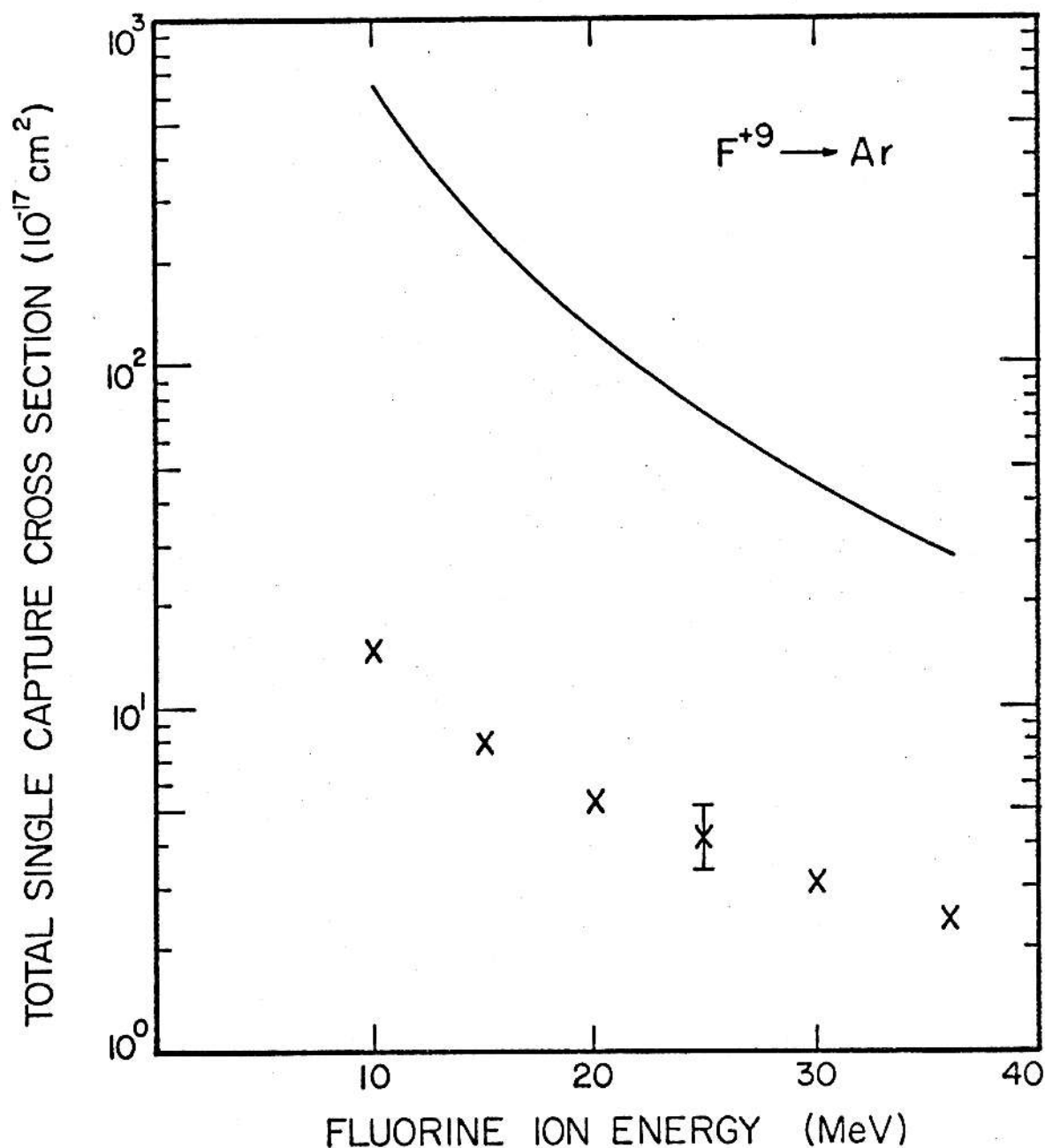
Experimental and calculated electron capture cross sections. The experimental values of the cross section for single capture are from Ref. 15 and 16 and the calculated cross sections are from Eq. (6).

TABLE II

Projectile	Energy (MeV)	$F^{+9}, O^{+8}, N^{+7}, C^{+6} \rightarrow Kr$		
		$\sigma_{exp.} (10^{-16})$	$\sigma_{calc.} (10^{-16})$	$\frac{\sigma_{calc.}}{\sigma_{exp.}}$
F^{+9}	10	1.55	126.20	81.41
	15	1.05	51.80	49.33
	20	.80	26.64	33.30
	25	.64	15.54	24.28
O^{+8}	10		60.70	
	15		24.34	
	20		12.38	
	25		7.194	
N^{+7}	10	.84	30.46	36.26
	15	.53	12.22	23.06
	20	.335	6.135	18.46
	25	.215	3.556	16.54
C^{+6}	10	.59	14.40	24.40
	15	.38	5.68	14.95
	20	.245	2.787	11.38
	25	.159	1.546	9.72

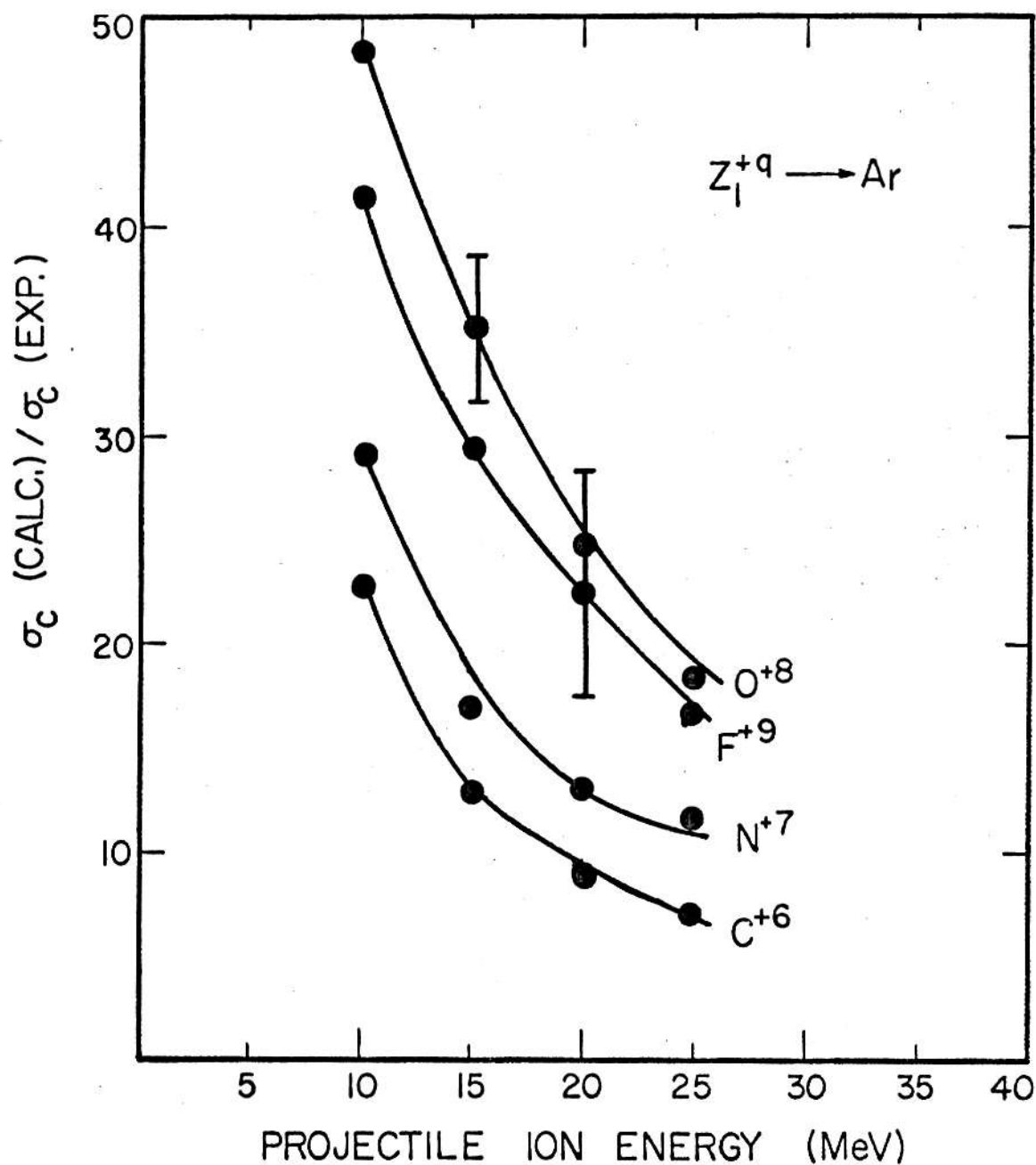
Experimental and calculated electron capture cross sections. The experimental values of the cross section for single capture are from Ref. 15 and the calculated cross sections are from Eq. (6).

FIGURE 16



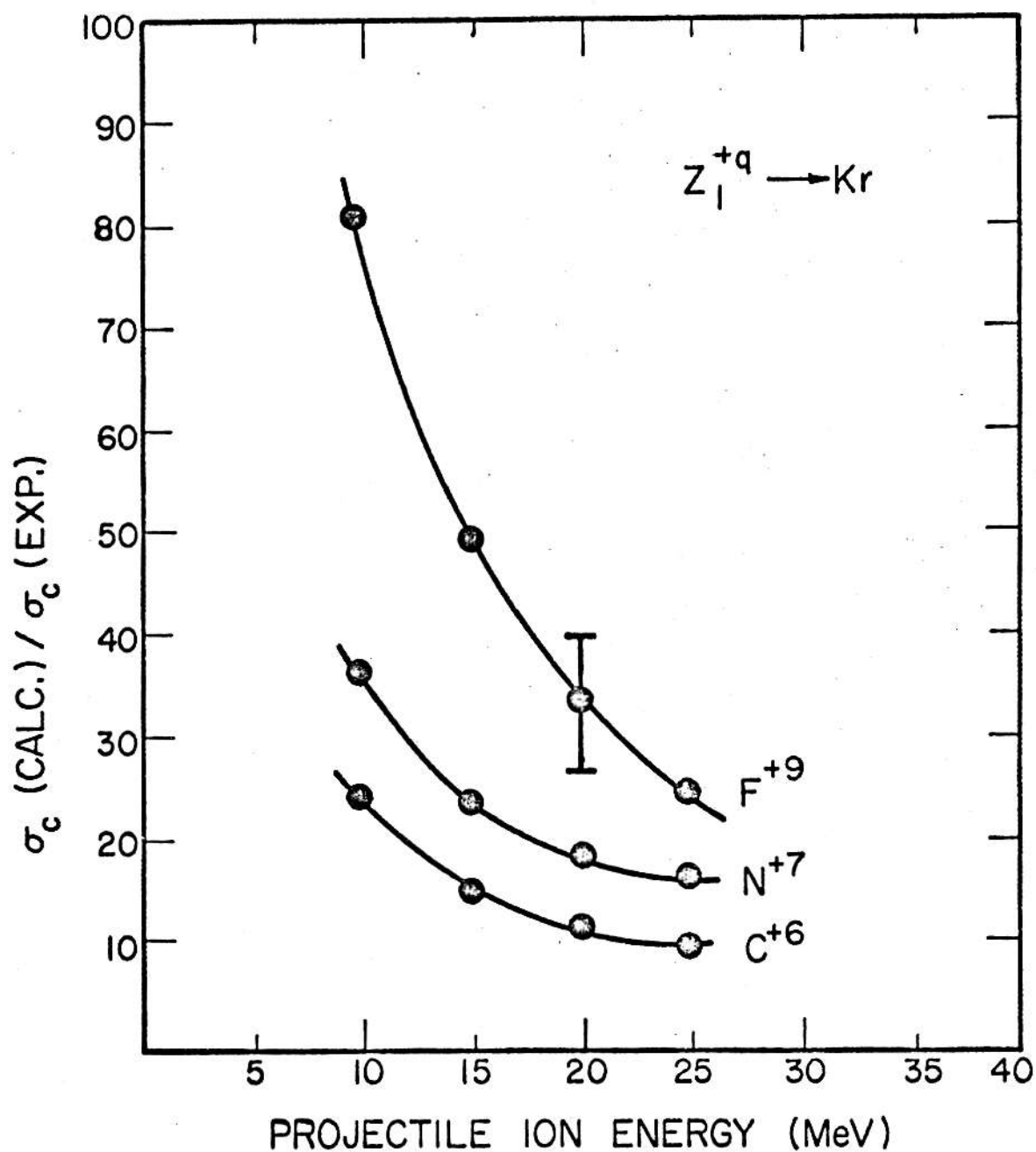
Total single capture cross section versus projectile energy for fluorine on argon. The experimental values from Ref. 15 are represented by the X's, while the calculated values from Eq. (6) are given by the solid line. The error bar represents the absolute error of the experiment.

FIGURE 17



Calculated-to-experimental single capture cross section ratios versus projectile energy for Z_l^{+q} on argon. The experimental values are from Ref. 15 and 16, while the calculated values are from Eq. (6). The solid line is to guide the eye and the error bars represent the absolute error in each of the experiments.

FIGURE 18

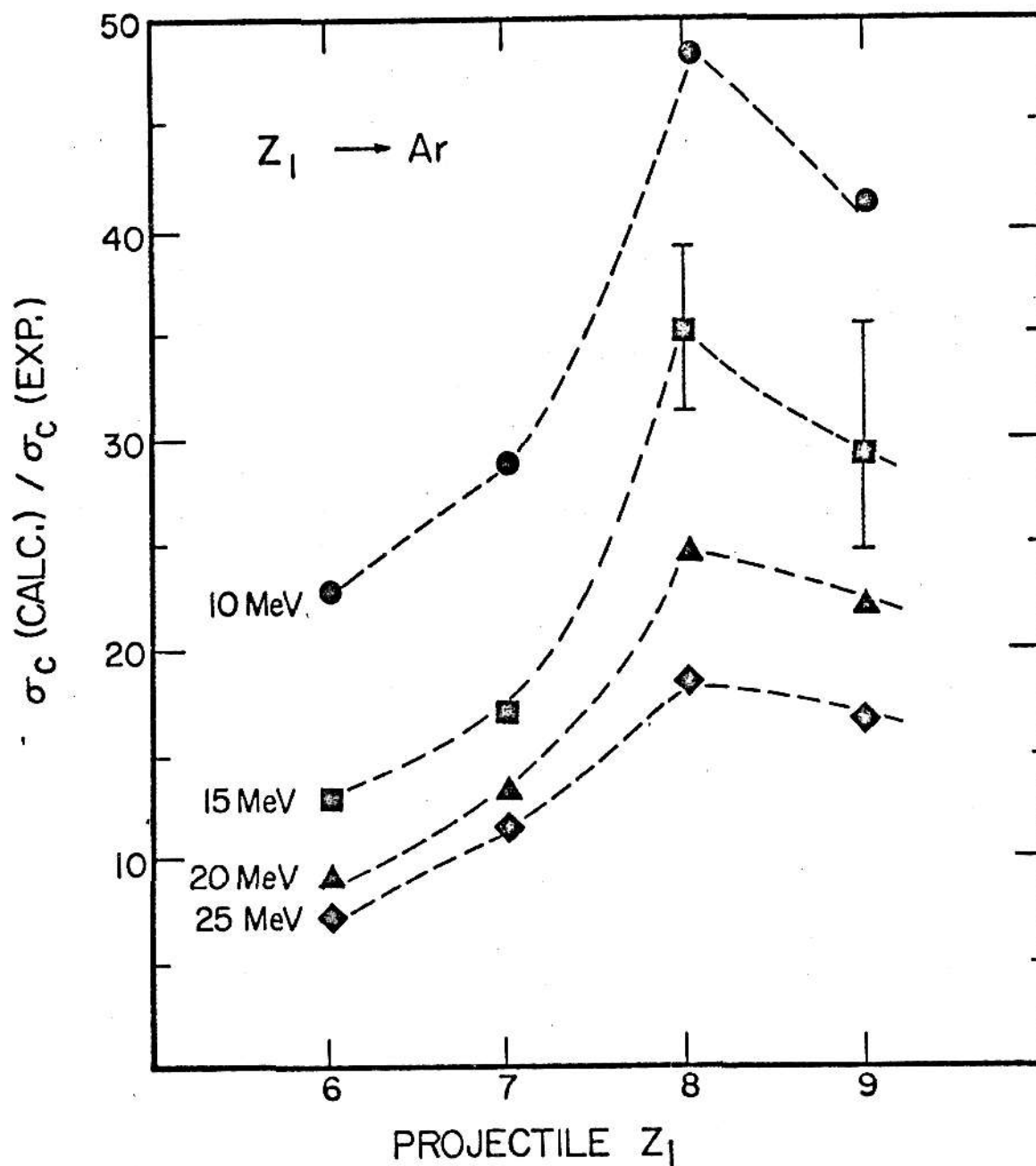


Calculated-to-experimental single capture cross section ratios versus projectile energy for Z_1^{+q} on krypton. The experimental values are from Ref. 15, while the calculated values are from Eq. (6). The solid line is to guide the eye and the error bar represents the absolute error in the experiment.

30% too high due to some systematic error, then the increase in the ratio of calculated to experimental cross section with increasing Z_1 is indicative that the Z_1 dependence in the calculation is too strong. The trends shown in these figures should be taken into account in any attempt to produce a fitting function for Eq. (6) as Nikolaev has done for protons.

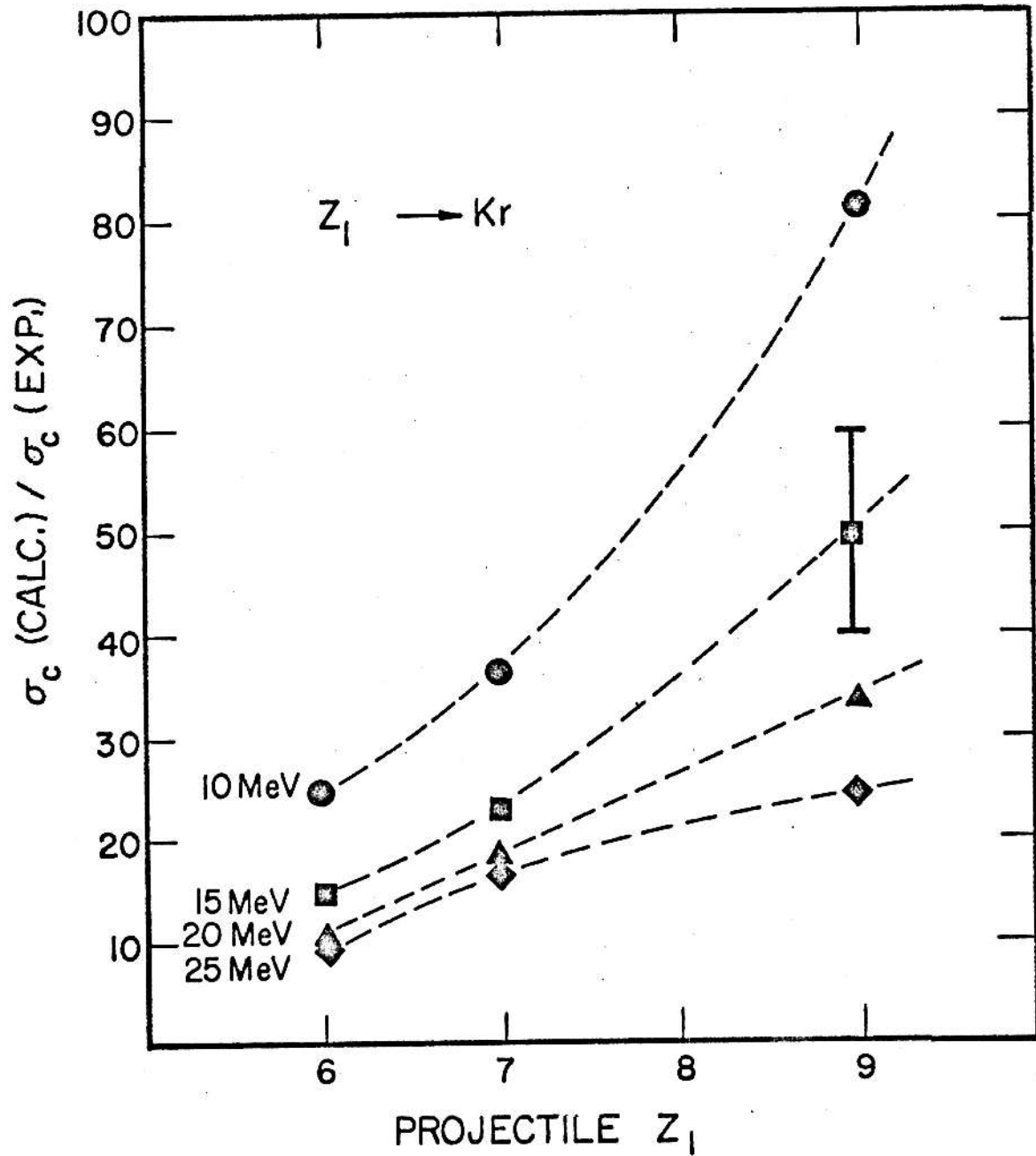
As expected from the comparison of cross sections with protons the absolute value of the calculated cross sections for these heavy ion capture reactions are too large. Surprisingly, however, the overestimate ranges from 6 to 80 times, monotonically decreasing with increasing projectile energy. Because of the gross overestimate of the calculation investigation of other trends require that a normalization be taken into account in order to interpret the results. These trends will be discussed in section IIID.

FIGURE 19



Calculated-to-experimental single capture cross section ratios versus projectile atomic number for Z_1 on argon. The experimental values are from Ref. 15, while the calculated values are from Eq. (6). The error bar represents the absolute error in the experiment.

FIGURE 20



Calculated-to-experimental single capture cross section ratios versus projectile atomic number for Z_1 on krypton. The experimental values are from Ref. 15, while the calculated values are from Eq. (6). The error bar represents the absolute error in the experiment.

C. Capture From a Particular Shell of the Target by Protons

As mentioned in section IIC an experiment has been done by Macdonald¹⁸ et al. to measure the cross section for capture specifically from the K shell of argon by energetic protons. The results of this experiment are listed in Table III along with the calculated values of Eq. (6). The calculated cross sections for capture from the K shell are seen to be between 4 and 5 times larger than the experimental values for the energy range of the experiment. This overestimate of the calculation is consistent with the results of section IIIA for the total capture cross sections by protons. These latter values can be used as away to normalize the calculated cross sections for capture from the K shell, $\sigma_{CK}(\text{calc.})$. The values scaled to total cross sections given in Table III are $\sigma_{CK}(\text{calc.}) \div (\sigma_{CT}(\text{calc.})/\sigma_{CT}(\text{exp.}))$ and are approximately a factor of two lower than the experimental values as is shown in a plot of the data in Fig. 21. However, the trend of the cross section as a function of energy is rather well represented by the normalized calculation.

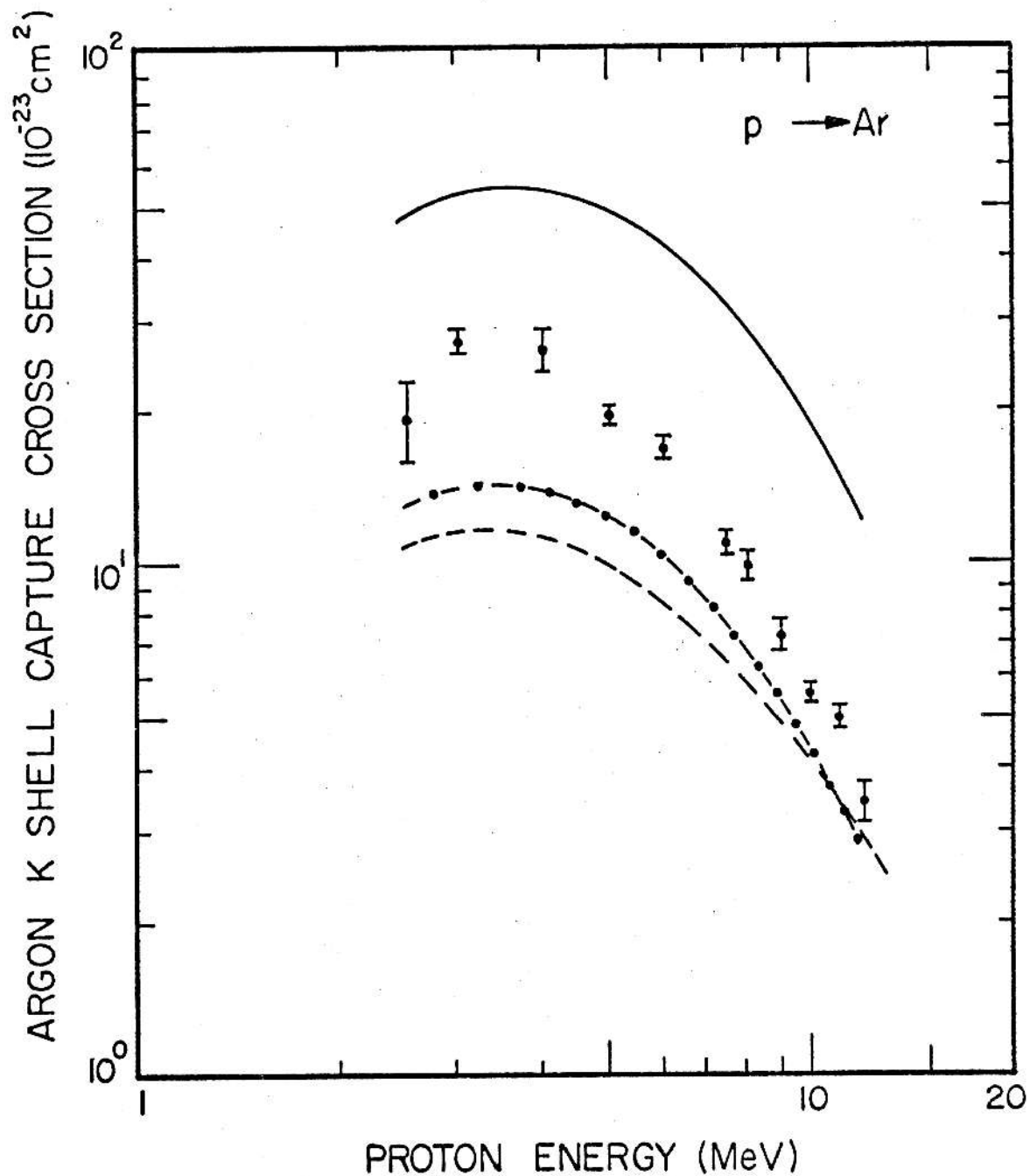
One may also use Nikolaev's $R_0(t)$ fitting function, Eq. (8), in order to obtain calculated cross sections which give approximately the same results for the scaled $\sigma_{CK}(\text{calc.})$. These results are also shown in Fig. 21 and the similar agreement using the two normalization technique is perhaps surprising since the $R_0(t)$ fitting function was determined using data from much lower energy proton beams which capture very much lower binding energy electrons (ie. at 2MeV, K shell, L shell, M shell capture from argon are respectively 0.1%, 90% and 10% of the total capture cross section).

TABLE III

Energy keV	$\frac{\text{EXP.}}{\sigma_{\text{CT}}}$ (10^{-24})	σ_{CK}	$\frac{\text{CALC.}}{\sigma_{\text{CT}}}$ σ_{CK} (10^{-24})	$\frac{\sigma_{\text{CT}}(\text{calc.})}{\sigma_{\text{CT}}(\text{exp.})}$	Scaled $\sigma_{\text{CK}}(\text{calc.})$ (10^{-24})
2.5	3840.0	19.2	17080.0	4.45	10.8
3.0	1942.0	27.2	8937.0	4.60	11.5
4.0	623.8	26.2	3007.0	4.82	11.2
5.0	257.8	19.6	1227.0	4.76	10.3
6.0	112.0	16.8	575.9	5.14	8.1
7.5	49.8	11.0	224.9	4.52	7.0
8.0	40.4	9.9	171.3	4.24	6.7
9.0	22.3	7.2	104.5	4.69	4.9
10.0	16.0	5.6	67.4	4.20	4.5
11.0	11.3	5.0	45.6	4.04	3.8
12.0	7.2	3.4	32.0	4.42	2.8

Experimental and calculated cross sections for 2.5 to 12 MeV protons on argon. The experimental values for the total capture cross sections, σ_{CT} , and the cross section for capture from the K shell of argon, σ_{CK} , are from Ref. 18; while the calculated values are from Eq. (6). Also listed is the calculated-to-experimental total capture cross section ratios, $\sigma_{\text{CT}}(\text{calc.})/\sigma_{\text{CT}}(\text{exp.})$, and the scaled calculated cross section for capture from the K shell.

FIGURE 21



Argon K shell capture cross sections versus proton energy. The various quantities shown are: •, the experimental values from Ref. 18; —, the calculated values from Eq. (6); ----, the scaled calculated values from Table III; -·-·-, and the calculated values using Eq. (4).

This comparison between the experimental and Brinkman-Kramers cross sections for K shell capture from argon has shown that the calculated values have the correct dependence on the proton energy. If the ratios of the calculated total capture cross sections to the experimental total capture cross sections are used to scale the calculated cross section for capture from a specific shell, the absolute experimental values are underestimated by less than a factor of two.

D. Capture to a Particular Shell(s) of the Projectile

As discussed in section IID, an experiment that has been done that permits a comparison with the calculated values of the cross section for capture to particular projectile shells using Eq. (6) is for F^{+9} on Ar. In this experiment the cross sections for K shell x ray production of the fluorine ion were determined by observing K shell radiation in a proportional counter. While it is true that any projectile radiation observed must be the consequence of a capture process, there are some capture events which do not result in a K shell x ray. For example, if the capture is to the ground state of the fluorine ion no radiation will result. Also, if the decay time for a transition from an excited state formed following capture is longer than the $\sim 2-5$ nsec viewing time of the x ray detection system the radiation will not be observed. For fluorine nuclei capturing electrons, the 2s state with a lifetime of $\sim 230^{26}$ nsec or states with $n_1 > 11$ will not decay within view of the detector. The determination of the fraction of electrons captured into excited states which do result in a K shell x ray depends not only on an understanding of the branching ratios of the decay channels of the projectile, but also on a knowledge of the population of the sublevels of each shell of the projectile. Although a Brinkman-Kramers calculation could be formulated to determine substate populations, the lack of experimental data for comparison precluded the cumbersome calculation that would be required.

In order to make comparisons with experimental cross sections and theoretical capture cross sections, it is necessary to estimate what fraction of the capture to excited states will result in x-ray transitions. For example, the theoretical branching ratios for hydrogenic decay to the 2s state show

that 12% of all decaying p states (with $n_1 > 2$) decay to the 2s state, and therefore only 88% of those electrons which are captured into $n_1 > 2$ will result in a fluorine K shell x ray. For $n_1 = 2$ it has been assumed that the electrons are captured with equal probability into each of the eight substates; two $^2S_{1/2}$ substates, two $^2P_{1/2}$ substates, and four $^4P_{3/2}$ substates. As stated previously, any electron in the 2s states will not produce observable radiation and, therefore, only 75% of those electrons captured into the $n_1 = 2$ state of the fluorine ion will result in a K shell x ray. In terms of Eq. (6) the cross section for the production of fluorine K shell x rays is given by this model as

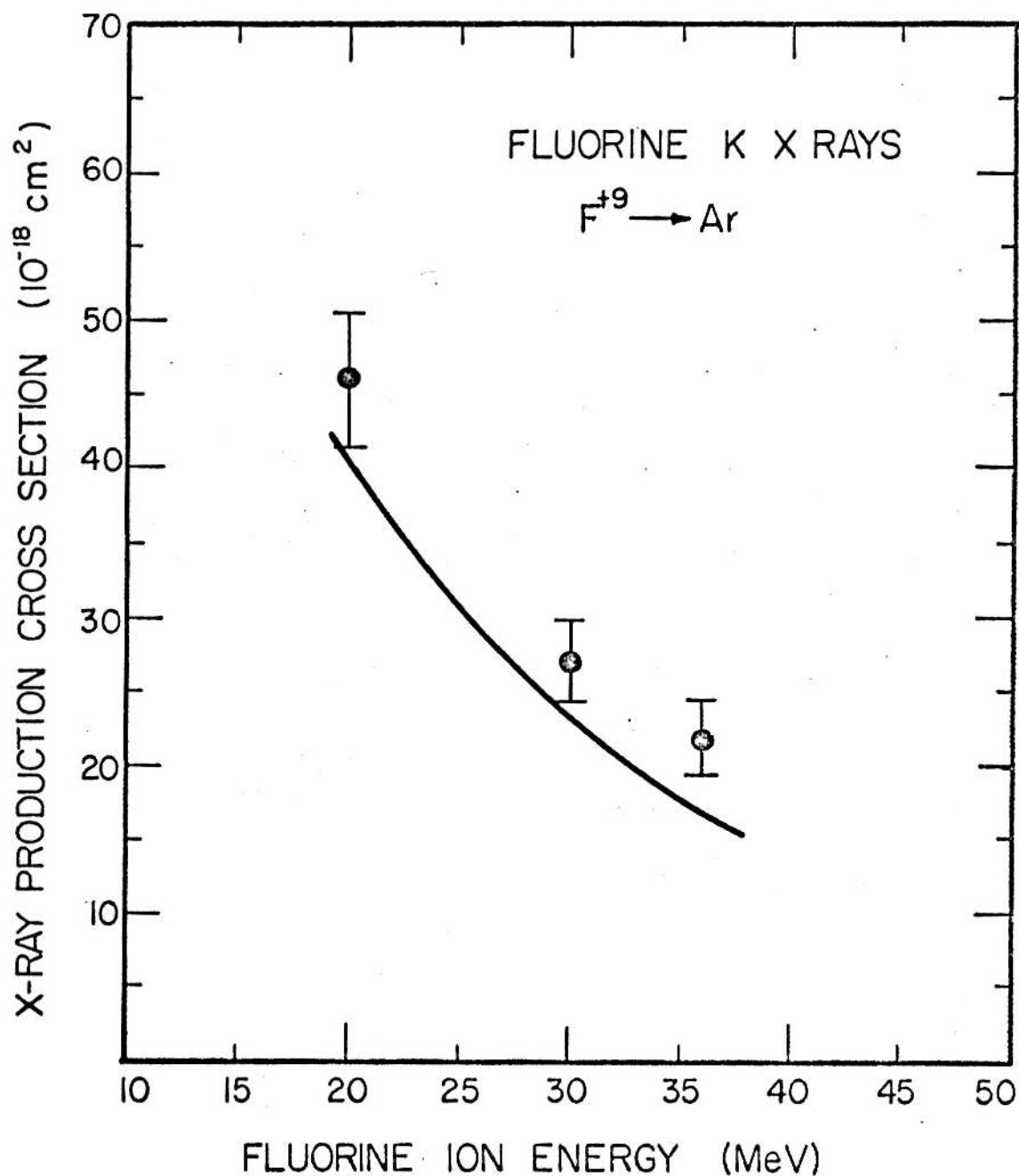
$$\sigma_{\text{XK}} = 88\% \left[\sum_{n_1 > 2, n_2} \sigma(n_1, n_2) \right] + 75\% \left[\sum_{n_2} \sigma(2, n_2) \right] \quad (19)$$

In this analysis no correction has been made to account for capture into $n_1 > 11$ since the cross section for these events is small compared to the cross section for capture into all states. That is, the ratio of $\sum_{n_1 > 11} \sigma(n_1, n_2) / \sum_{n_1, n_2} \sigma(n_1, n_2)$ is $\sim 5\%$ and, therefore, neglecting these events does not introduce an appreciable error in the calculated values of the cross sections.

In section IIIB it was seen that the calculated values for the total single capture cross section were much larger than the experimental values and the ratio of the calculated to experimental value was formed for different energies. These ratios are now used as normalization factors to lower the calculated values of Eq. (19), which consists of a sum of cross sections from Eq. (6), for the cross section for K shell x-ray production of the fluorine ion. The normalized cross section is $\sigma_{\text{XK}}(\text{calc.}) \left(\frac{\sigma_{\text{CT}}(\text{calc.})}{\sigma_{\text{CT}}(\text{exp.})} \right)^{-1}$

The results for the normalized cross sections of Eq. (19) and the experimental results for the K shell x-ray production is shown in Fig. 22 where both the experimental and calculated values are plotted as a function of projectile energy. The agreement of the normalized calculated cross sections with the observed values is rather remarkable. In other words, the predictions of the calculation (Eq. 19)), when normalized to the total single capture cross sections, are in better agreement with the experimentally measured x-ray production cross sections than might be anticipated from the approximations made in the theoretical model.

FIGURE 22



Projectile x-ray production cross section versus projectile energy for fluorine on argon. The experimental values, with their relative error bars, are from Ref. 20 and are represented by the \bullet 's; while the calculated values from Eq. (19) are given by the solid line.

SUMMARY

Calculated cross sections for electron capture have been obtained from the modified Brinkman-Kramers calculation of Nikolaev¹² with the facilitation of a computer program. These theoretical values have been compared to experimental data for a variety of systems; $p \rightarrow \text{Ar}$, N_2 , Ne , He , H_2 and F^{+9} , O^{+8} , N^{+7} , $\text{C}^{+6} \rightarrow \text{Ar}$ and Kr . For the cases with protons as projectiles, the calculated values are 3-5 times too large when compared to experiments of Welsh et al.²¹, but do have the correct energy dependence. For the heavy projectile cases, the overestimates of the calculation increase dramatically to overestimate the experimental cross sections by factors of 6-80 in the energy range studied. Again, the calculated values give a reasonable energy dependence when compared to the experimental values of Chiao¹⁵. However, it was found that the overestimation of the calculation increases with increasing projectile atomic number and decreasing projectile energy. Any improvement in the theory of the electron capture process must take into account these variations.

In order to compare the results of the calculation to other experimental processes which are connected to electron capture events, the ratios of calculated-to-experimental total single capture cross section were used as normalization factors. When normalized in this manner, it was found that the calculated cross sections for capture from the K shell of argon by protons were within a factor of two of the experimental values given by Macdonald et al.¹⁸ Lastly, the normalized calculated cross sections for x-ray emission following electron capture in argon to excited states of fluorine projectiles were compared to the experimental values of Brown et al.²⁰ The results of such a comparison show good agreement between the experimental and theoretical

values for the cross sections for K shell x-ray production from the fluorine ions.

It has been demonstrated that the elementary calculation of the electron capture process using the Brinkman-Kramers approximation can be useful in interpreting experimental data connected with capture events. The formula used is derived for a one-electron transfer from closed shell targets to bare projectiles and does not give information about substates in the system. However, the fact that it is in closed form makes it attractive as a tool in analyzing trends in experimental data.

APPENDIX

ILLEGIBLE DOCUMENT

**THE FOLLOWING
DOCUMENT(S) IS OF
POOR LEGIBILITY IN
THE ORIGINAL**

**THIS IS THE BEST
COPY AVAILABLE**

BRINKMAN-KRAMERS CALCULATION FOR CAPTURE CROSS-SECTION FROM NIKOLAEV EQUATION # 6

```

K= NUMBER OF ELECTRONS IN TARGET SHELL, I= LEVEL OF EJECTED EL
N1= LEVEL OF CAPTURED ELECTRON
D=BETA , F= RATIO OF PROJ. VEL. TO TARGET ELECTRON VEL. ,
H= GAMMA , W(N1) = SIGMA TIMES N1 CUBED , X= LOG W(N1)
AI =PHI_4, I_=# OF ELEC. IN _ SHELL OF TARGET
DIMENSION B(3),Z2(3),SIGMA(100,100),W(100)
R=0.0
ISHEL=2
IK=2
IL=8
IM=0
L=12
M=1
30 FORMAT(3F6.2,6F7.2,2F6.2)
50 FORMAT(1H1,'ENERGY =',F6.2,'MEV',10X,'Z OF PROJ. =',F6.2,
  C10X,'M OF TARGET =',F6.2,'AMU',10X,'MASS OF PROJ. =',F6.2,')
60 FORMAT(1H0,3X,'Z2*(N2)',6X,'N2',10X,'SIGMA',7X,'W(N1)',
  C9X,'X',8X,'B(N2)',9X,'N1',14X,'BETA',6X,'GAMMA',10X,'R')
70 FORMAT(1H0,2X,F6.2,6X,I3,6X,1PE10.3,3X,1PE10.3,3X,1PE10.3,3X,
  C1PE10.3,3X,I3,8X,1PE10.3,3X,1PE10.3,3X,1PE10.3)
80 FORMAT(1H0,3X,'SIGMA FROM ALL SHELLS TO SHELL #',I3
  C,3X,'OF PROJ. =',1PE10.3)
90 FORMAT(1H0,3X,'SIGMA TOTAL ALL TO ALL =',1PE10.3)
100 FORMAT(1H0,3X,'SIGMA FROM SHELL #',I3,
  C3X,'TO ALL SHELLS PROJ. =',1PE10.3)
110 FORMAT(1H0,3X,'SIGMA FROM SHELL #',I3,
  C3X,'TO EXCITED SHELLS ONLY =',1PE10.3)
120 FORMAT(1H0,3X,'SIGMA FROM ALL TO EXCITED STATES ONLY =',1PE10.3)
121 FORMAT(1H0,'THE RATIO OF K-CAPTURE',1PE10.3,' TO THE TOTAL
  CCAPTURE',1PE10.3,' IS',1PE10.3,' PERCENT')
125 FORMAT(1H0,'ENERGY =',F6.2,'MEV',10X,'Z OF PROJ. =',F6.2,
  C10X,'M OF TARGET =',F6.2,'AMU',10X,'MASS OF PROJ. =',F6.2)
10 K=IK
  I=1
  READ(5,30) E,Z1,Z2T,B(1),B(2),B(3),Z2(1),Z2(2),Z2(3),AMAS1
  WRITE(6,50) E,Z1,Z2T,AMAS1
  WRITE(6,60)
11 A=(R(I)/13.6)**.5
  BB=(E/(AMAS1*.024975))**.5
  C=Z2(I)/I
  D=((C/A)**2)-1.0
  CONST=1.12E-16
  F=BB/A
  DO 17 N1=1,10
12 G=Z1/(N1*A)
  H=4.0*(F**(-2))*(1.0+2.0*(1.0+G**2)*(F**(-2)))+(1.0-(G**2))
  C**2*(F**(-4))**(-1)
  AK=(1.0+D)**2.5
  AL=1.0/(1.0+D*H)**3
  IF(D*H-1)13,13,14
13 AI=(1-.25*D*H)
  GO TO 15
14 AI=1.0/(1.0+D*H)**.46
15 P=AK*AL*AI
  SIGMA(N1,I)=(CONST*K*(H*Z1)**5*P)/(A**5*N1**3*(E/AMAS1))
  W(N1)= SIGMA(N1,I)*N1**3
  X=ALOG(W(N1))

```



```

      WRITE(6,70) Z2(I),1,SIGMA(N1,I),W(N1),X,B(I),N1,D,H,R
17  CONTINUE
      IF (I-1) 31,32,31
32  IF (I-ISHEL) 33,20,33
33  K=IL
      GO TO 19
31  IF(I-2) 81,34,31
34  IF (I-ISHEL) 35,20,35
35  K=IM
      GO TO 19
81  IF(I-3) 20,82,20
82  IF(I-ISHEL) 83,20,83
83  K=IN
19  I=I+1
      N1=I
      GO TO 11
20  SUM=0.0
      DO 54 N1=1,10
      FATP=0.0
      DO 44 I=1,ISHEL
      FATP=FATP+SIGMA(N1,I)
44  CONTINUE
      WRITE(6,80) N1,FATP
      SUM=SUM+FATP
54  CONTINUE
      WRITE(6,90) SUM
      TOM=0.0
      DO 74 I=1,ISHEL
      FPTA=0.0
      DO 64 N1=1,10
      FPTA=FPTA+SIGMA(N1,I)
64  CONTINUE
      WRITE(6,100) I,FPTA
      FPTE=FPTA-SIGMA(1,I)
      WRITE(6,110) I,FPTE
      TOM=TOM+FPTE
74  CONTINUE
      WRITE(6,120) TOM
      FKTA=0.0
      DO 65 N1=1,10
      FKTA=FKTA+SIGMA(N1,1)
65  CONTINUE
      RKTT=(FKTA/SUM)*100.0
      WRITE(6,121) FKTA,SUM,RKTT
      WRITE(6,125) F,Z1,Z2T,AMAS1
      IF(L-M) 21,21,22
22  M=M+1
      GO TO 10
21  CONTINUE
      RETURN
      END

```

TABLE IV

Target Atom	Z*(1)	Z*(2)	Z*(3)	Z*(4)	B(1)	B(2) (eV)	B(3)	B(4)
H	1.00	-	-	-	13.60	-	-	-
He	1.69	-	-	-	24.59	-	-	-
N	6.67	3.84	-	-	403.00	16.85	-	-
Ne	9.70	5.86	-	-	867.00	21.50	-	-
Ar	17.51	13.56	7.01	-	3206.30	268.52	19.18	-
Kr	35.70	31.80	19.80	10.16	14327.00	1750.00	153.00	17.55

Table of the values used in the computer program for the evaluation of cross sections from Eq. (6) from Refs. 13 and 14.

LIST OF REFERENCES

1. A summary of experiments involving the measurements of inelastic energy loss for a variety of collision systems is given by Q. C. Kessel, in Case Studies in Atomic Collision Physics, E. W. McDaniel and M. R. C. McDowell (North-Holland, New York, 1969), Vol. 1, p.412.
2. J. D. Garcia, Phys. Rev. A 1, 280 (1970), *ibid.* 1402 (1970) and E. Merzbacher and H. W. Lewis, in Encyclopedia of Physics, S. Flugge (Springer-Verlag, Berlin, 1958), Vol. 34, p.166.
3. M. R. C. McDowell and J. P. Coleman, Introduction to the Theory of Ion-Atom Collisions, (North-Holland, Amsterdam, 1970), chap. 8.
4. D. R. Bates and A. Dalgarno, Proc. Phys. Soc. (London) A65, 919 (1952).
5. J. D. Jackson and H. Schiff, Phys. Rev. 89, 359 (1953).
6. R. H. Bassel and E. Gerjuoy, Phys. Rev. 177, 749 (1960).
7. T. B. Day, L. S. Rodberg, G. A. Snow, and S. Sucher, Phys. Rev. 123, 1051 (1961).
8. J. R. Oppenheimer, Phys. Rev. 31, 349 (1928).
9. H. C. Brinkman and H. A. Kramers, Proc. Acad. Sci. (Amsterdam), 33, 973 (1930).
10. R. A. Mapleton, Phys. Rev. 130, 1829 (1963).
11. H. D. Betz, Rev. Mod. Phys. 44, 465 (1972).
12. V. S. Nikolaev, Soviet Phys.-JETP 24, 847 (1967).
13. W. Lotz, Jour. of Opt. Soc. Am. 60, 206 (1970).
14. E. Clementi and D. L. Raimondi, J. Chem. Phys. 38, 2686 (1963).
15. T. Chiao, PhD. thesis (Kansas State University, 1973).
16. J. R. Macdonald and F. W. Martin, Phys. Rev. A 4, 1965 (1971).

17. S. M. Ferguson, J. R. Macdonald, T. Chiao, L. D. Ellsworth, and S. A. Savoy, Phys. Rev. A 8, 2417 (1973).
18. J. R. Macdonald, C. L. Cocke, and W. W. Eidson, Phys. Rev. 32, 648 (1974).
19. L. M. Winters, J. R. Macdonald, M. D. Brown, L. D. Ellsworth, and T. Chiao, Phys. Rev. A 7, 1276 (1973).
20. M. D. Brown, L. D. Ellsworth, J. A. Guffey, T. Chiao, E. W. Pettus, L. M. Winters, and J. R. Macdonald, to be published in Phys. Rev. A (Oct. 1974).
21. L. M. Welsh, K. H. Berkner, S. N. Kaplan, and R. V. Pyle, Phys. Rev. 158, 158 (1967).
22. A. M. Halpern and J. Law, Phys. Rev. Letters 31, 4 (1973).
23. Review article by S. K. Allison and M. G. Munoy in Atomic and Molecular Processes, D. R. Bates (Academic Press, Inc., New York, 1962).
24. H. Schiff, Can. J. Phys. 32, 393 (1954).
25. R. M. May and J. Lodge, Phys. Rev. 137A, 699 (1965).
26. R. A. Marrus, Nucl. Inst. and Meth. 110, 333 (1973).
27. P. J. Kramers, Phys. Rev. A 6, 21 (1972).
28. J. H. McGuire, Phys. Rev. A 8, 2760 (1973).
29. V. S. Nikolaev, Soviet Phys.-Usp 8, 269 (1965).
30. S. K. Allison, Rev. Mod. Phys. 30, 1137 (1958).
31. D. R. Bates, Proc. Roy. Soc. (London) A247, 2941 (1958).
32. I. M. Cheshire, Proc. Phys. Soc. (London) 84, 89 (1964).
33. R. H. Hughes, C. A. Stigers, B. M. Doughty, and E. D. Stokes, Phys. Rev. A 1, 1424 (1970).
34. E. H. Pedersen, S. J. Czuchlewski, M. D. Brown, L. D. Ellsworth, and J. R. Macdonald, to be published.

35. Recent preliminary results³⁴ indicate that the fluorine K shell radiation following electron capture by 33MeV F^{+9} ions is somewhat anisotropic. If such anisotropy exists for the other experiments described in this work, the reported cross sections will be systematically high. However, the interpretation of the data are not expected to change since the correction of a few percent needed would be within any uncertainty inherent in the calculation.

A COMPARISON BETWEEN EXPERIMENTAL ELECTRON
CAPTURE DATA AND A MODIFIED BRINKMAN-KRAMERS CALCULATION

by

JAMES ANDREW GUFFEY

B. S., University of Missouri-St. Louis, 1972

AN ABSTRACT OF A MASTER'S THESIS

submitted in partial fulfillment of the

requirement for the degree

MASTER OF SCIENCE

Department of Physics

KANSAS STATE UNIVERSITY
Manhattan, Kansas

1974

ABSTRACT

In this thesis single electron capture cross sections for the systems $p \rightarrow \text{Ar, Ne, N}_2, \text{He, H}_2$ and $\text{F}^{+9}, \text{O}^{+8}, \text{N}^{+7}, \text{C}^{+6} \rightarrow \text{Ar and Kr}$ have been obtained in a Brinkman-Kramers type formulation as given by Nikolaev¹. These calculated values have been compared to experimental data for total single capture cross sections as well as x-ray production cross sections representing capture from particular shells of the target or to excited states of the projectile. It is found that the overestimate of the calculated cross section magnitude increases with increasing projectile atomic number and with decreasing projectile velocity. However, when the calculated values for each system are normalized to experimental total single capture cross sections then the Brinkman-Kramers theory does give values for the cross sections from particular shells and to excited states which are in good agreement with experiment.

1) V. S. Nikolaev, Soviet Phys. JETP 24, 847 (1967).